General Disclaimer

One or more of the Following Statements may affect this Document

- This document has been reproduced from the best copy furnished by the organizational source. It is being released in the interest of making available as much information as possible.

- This document may contain data, which exceeds the sheet parameters. It was furnished in this condition by the organizational source and is the best copy available.

- This document may contain tone-on-tone or color graphs, charts and/or pictures, which have been reproduced in black and white.

- This document is paginated as submitted by the original source.

- Portions of this document are not fully legible due to the historical nature of some of the material. However, it is the best reproduction available from the original submission.

NASA

Technical Memorandum 85125

PERFORMANCE APPRAISAL OF VAS RADIOMETRY FOR GOES-4, -5 AND -6

Dennis Chesters and
Wayne D. Robinson

DECEMBER 1983

National Aeronautics and
Space Administration

Goddard Space Flight Center
Greenbelt, Maryland 20771

PERFORMANCE APPRAISAL OF VAS RADIOMETRY

FOR GOES-4, -5 AND -6

by

Dennis Chesters

Goddard Laboratory for Atmospheric Sciences

NASA/Goddard Space Flight Center

Greenbelt, Maryland 20771

and

Wayne D. Robinson

General Software Corporation

Landover, Maryland 20785

December, 1983

ABSTRACT

The first three VISSR Atmospheric Sounders (VAS) were launched on GOES-4, -5 and -6 in 1980, 1981 and 1983. Postlaunch radiometric performance is assessed for noise, biases, registration and reliability, with special attention to calibration and problems in the data processing chain.

The postlaunch performance of the VAS radiometer meets its prelaunch design specifications, particularly those related to image formation and noise reduction. The best instrument is carried on GOES-5, currently operational as GOES-EAST. Single-sample noise is lower than expected, especially for the small longwave and large shortwave detectors. Detector-to-detector offsets are correctable to within the resolution limits of the instrument. Truncation, zero-point and droop errors are insignificant. Absolute calibration errors, estimated from HIRS and from radiation transfer calculations, indicate moderate, but stable biases. Relative calibration errors from scanline to scanline are noticeable, but meet sounding requirements for temporally and spatially averaged sounding fields-of-view.

The VAS instrument is a potentially useful radiometer for mesoscale sounding operations. Image quality is very good. Soundings derived from quality controlled data meet prelaunch requirements when calculated with noise- and bias-resistant algorithms. The information from the mid- and low-level channels is better than expected. Good results have even been obtained at 16x16 km^2 resolution, and useful work seems possible at 8x8 km^2 resolution. The information content of the faint, noisy upper air channels remains scientifically untested. While the distant geosynchronous station of the VAS instrument makes accurate radiometry difficult, the frequent and relatively stable measurements which VAS provides at fixed angle and resolution permits mesoscale measurements which were previously unavailable.

CONTENTS

LIST OF FIGURES

LIST OF TABLES

Section 1

INTRODUCTION

During the 1970s, the Visible Infrared Spin-Scan Radiometer (VISSR) was carried on the SMS/GOES series of geosynchronous satellites. The original VISSR instrument formed infrared images in the 11 μm window by stepping one scanline per spin. During the early 1980s, the GOES-4, -5 and -6 satellites are carrying an upgraded instrument called the VISSR Atmospheric Sounder (VAS). The most significant improvements are the addition of eleven more infrared channels with an order-of-magnitude improvement of the internal calibration. VAS was designed to meet the requirements of observing the development of subsynoptic and mesoscale temperature and moisture distributions. From geosynchronous station, VAS can survey the United States with 12 spectral bands once per hour at approximately 30 km resolution. Image sequences in a few channels can be acquired even more frequently in order to produce time-lapse observations of rapidly developing weather systems. Relatively accurate data are required for multispectral images of the structure and changes in the atmosphere, and very accurate radiances are required for the retrieval of temperature and moisture profiles.

The VAS instrument was developed by NASA for NOAA in a decade-long project known as the VAS Demonstration (Montgomery, 1980). The main goals of the VAS Demonstration were to build and launch the instrument, to develop ground systems for the data, and to produce some useful images and soundings. Prelaunch assessments of the VAS radiometry meet specifications (Malinowski and Ruis, 1980; Menzel, 1980). The first postlaunch asessments were based upon the VAS-D instrument on GOES-4 (Chesters et al., 1981; Menzel et al., 1981; Smith et al., 1981). The first VAS instrument performed adaquately, despite initial problems with the ground system, a malfunctioning detector, and eventual failure of the scan mechanism. The absolute calibration errors on GOES-4 were significantly biased to low values, as determined by comparison to radiation transfer calculations and to measurements from the HIRS instrument. These errors were relatively stable, so that soundings were possible with bias-compensated algorithms. All three VAS instruments have been evaluated by the contractors for pre- and post-launch radiometric performance (Menzel, 1980, 1981a, 1981b, 1981c, 1983a and 1983b). The VAS instrument on GOES-5 has provided most of the data for testing by users, who find the radiances to be useful for image sequences and sounding purposes (Greaves, 1983; Lee et al., 1983; Smith, 1983; Menzel et al., 1983b). VAS postlaunch performance is also reviewed in the final report of the VAS Demonstration, which contains a summary of this manuscript and additional evaluations of detector-to-detector registration, spin budgets and absolute calibration accuracy (Chesters et al., 1984).

This report is a postlaunch radiometric evaluation of all three VAS instruments. VAS radiances are assessed from the point-of-view of the VAS sounding scientist, who must understand the quirks and limitations of the data in order to make optimal use of the measurements. Prelaunch specifications and instrumental characteristics are described. Various ground system features which affect radiometric quality are discussed. Radiometric quality is compared to prelaunch specifications, and limitations are identified in the VAS instrument and in the data processing system on the ground. Because of the difficulty in assessing the radiometric errors of a remotely based infrared instrument without external standards, most evaluations are made by comparing the relative variations within VAS radiances (between samples, lines, detectors, etc.). VAS performance is explicitly evaluated for: random noise and associated averaging requirements, truncation errors, zero-point errors, droop along a scanline, scan-to-scan reproducability, absolute calibration errors, "scattered light" and resampling errors, and ground system problems. The radiometric errors are reviewed for their impact upon atmospheric soundings.

Section 2

REVIEW OF VAS CHARACTERISTICS

2.1 THE VAS INSTRUMENT

The previous VISSR instrument provided visible images of the earth along with infrared data in a single 11 μm window channel (Bristor, 1975). The VAS instrument has expanded the previous infrared capability by providing 12 channels of radiometric data between 4 and 15 μm. The channels were chosen to distinguish among the effects of tropospheric temperature, moisture and cloud cover upon the upwelling radiances. All 12 channels can be operated at 13.8 km horizontal resolution (instantaneous geometrical field-of-view (IGFOV) at nadir). The brighter longwave channels can be operated using the small (6.9 km IGFOV) detectors which provide the operational VISSR 11 μm data. The radiometer has been upgraded to yield higher precision values (10 bits instead of 8) from redundant sensors (3 independent detector pairs instead of 1 redundant pair). VAS radiances are carefully calibrated with outer space (3 K) and an internal hot target (320 K). This calibration is accomplished by a ray-tracing model with empirical correction coefficients for the radiative contributions from the foreoptics components of the VAS telescope, whose temperatures are continuously monitored by the GOES system. Radiometric noise can be reduced by "dwell averaging" several spins on the same line and channel. The number of spins allocated to the channels is termed the "spin budget". Noise can also be reduced after data collection by judicious averaging of the clear adjacent fields-of-view. Considerable effort has gone into prelaunch development of VAS radiometry (Montgomery and Endres, 1977; Malinowski and Ruiz, 1980; Menzel, 1980).

TABLE 1

Design features of the VAS channels

VAS Ch. No.	Spectral Filters Center, μm	Center, cm^{-1}	Width cm^{-1}	Purpose for Sounding	Main Abs. Gas	Other Signif. Effects
1	14.73	678.7	10.	temp	CO_2	O_3
2	14.48	690.6	16.	temp	CO_2	O_3
3*	14.25	701.6	16.	temp	CO_2	O_3
4*	14.01	713.6	20.	temp	CO_2	O_3
5*	13.33	750.	20.	temp	CO_2,H_2O	O_3
6	4.525	2210.	45.	temp+cloud	N_2O	Sun
7*	12.66	790.	20.	moisture	H_2O	CO_2+dust
8*	11.17	895.	140.	surface	H_2O	CO_2+dust
9*	7.261	1377.2	40.	moisture	H_2O	CO_2
10*	6.725	1487.	150.	moisture	H_2O	-
11	4.444	2250.	40.	temp+cloud	N_2O,CO_2	Sun
12	3.945	2535.	140.	surface	H_2O	Sun+dust

* Available at 6.9 km as well as 13.8 km IGFOV.

Table 1 lists the general design features of the VAS channels (Montgomery and Endres, 1977). VAS channel 8 is the VISSR 11 μm window operated with the large detectors, and its view of the surface is significantly affected by molecular absorption from atmospheric water vapor and carbon dioxide. Each of the VAS bandpasses were selected with temperature, water vapor, surface and cloud detection in mind, based upon experience with the infrared sounders in polar orbit. The detailed spectral response (filter function) for each of the 12 VAS channels was measured prior to launch, and found to meet the center and width specifications which are listed in Table 1 (see Appendix A).

VAS calibration, noise, resolution and registration requirements were thoroughly reviewed before the first VAS launch (Montgomery and Endres, 1977; Menzel, 1980). Other important VAS characteristics are:

- The large detectors project as 0.384 mrad square IGFOVs (13.8 km horizontal resolution at nadir). The small detectors are approximately 0.192 mrad squares (6.9 km IGFOVs, slightly rectangular on GOES-5 and -6). East-west offsets between the detectors are corrected in software on the ground before VAS data is sent to the user.

- Successive infrared samples are autocorrelated by approximately 40% to 60% due to deliberate smoothing of the 1/f noise in the signal processing. Electronically independent measurements are available after 3 to 5 samples.

- VAS resolution is diffraction limited. Only 80% of the radiance observed with a large detector is collected from within the IGFOV. Approximately 90% is collected within a circle of radius 0.221 mrad (15.9 km diameter footprint at nadir). 99% is collected within a circle of radius 0.932 mrad, which is a diameter equal to 5 large detector IGFOVs (70.0 km diameter footprint at nadir). Geometrical projection further extends the footprint by 20% to 50% at the latitudes of the United States. Consequently, the horizontal resolution of VAS is not precisely defined. Consequently, values like 8 km and 16 km will be used to describe the resolution of the small and large detectors, respectively.

- The scan mirror takes steps of 0.192 mrad in the north-south direction, equal to the IGFOV for the small longwave detectors. A full-earth frame consists of 1821 steps.

- The GOES nominal spin rate is 100 revolutions per minute. Infrared detectors are sampled every 8 μsec, as the footprint travels 0.084 mrad. Hence, the large detector IGFOVs are oversampled by a factor of 4.6, and the small detectors by 2.3.

- Earth-location requirements are ±10.0 km absolute and ±1.4 km relative (±10% of a large detector's IGFOV) accuracy.

- Each spin-scan produces a scanline from the "upper" and "lower" detector of a pair. Each infrared scanline consists of 3822 radiometric samples, with each sample represented as a 10-bit positive integer. The 10-bit integers are converted into calibrated radiances by the data processing systems on the ground. Bit-error rates during data transmission should be less than 1 in 10^4. Bit errors in the transmitted infrared data are not correctable.

2.2 VAS SENSITIVITY TO TERRESTRIAL CONDITIONS

TABLE 2

Estimated sensitivity of the the VAS channels

VAS Ch. No.	Peak Resp. (mb)	10%-90% Radiance Layer (mb)	Std. Sensitivity (K/°C) Temp	Dewpt	Surf	Std. T* (K)	Conversion dR/dT* (erg/etc./K)
1	70	4-120	1.00	-.00	.00	219	0.9
2	125	4-225	.99	-.00	.00	219	0.9
3	200	15-475	.91	-.02	.00	223	1.0
4	500	40-900	.73	-.09	.02	238	1.2
5	920	420-surf	.47	-.30	.29	260	1.5
6	850	520-surf	.43	-.03	.44	257	0.051
7	1000	720-surf	.33	-.37	.63	270	1.6
8	surf	920-surf	.17	-.20	.84	272	1.7
9	600	110-820	.82	-.70	.02	254	0.43
10	400	240-620	.94	-.70	.00	246	0.21
11	300	7-1000	.80	-.01	.04	237	0.013
12	surf	surf-surf	.08	-.03	.92	273	0.036

erg/etc. = erg/(sec cm^2 steradian cm^{-1}).

Table 2 lists the estimated sensitivity of the VAS channels for the U.S. Standard Atmosphere. The thickness of the central 80% radiance layer indicates the problem with assigning a radiance feature to the level of peak response. The channel sensitivites are estimated as the change in the calculated brightness temperature for a one degree change in the temperature or dewpoint of the entire standard profile or for a one degree change in surface (skin) temperature. The independent sensitivities present a problem with interpreting radiance variations within a single VAS channel. For instance, channel 5 at 13.3 μm is simultaneously sensitive to variations in air temperature, dewpoint and surface (skin) temperature. Several channels have nearly equal and opposite sensitivity to temperature and dewpoint, so that these channels are insensitive indicators of dewpoint depression. Table 2 also lists conversion factors between radiance and brightness temperature.

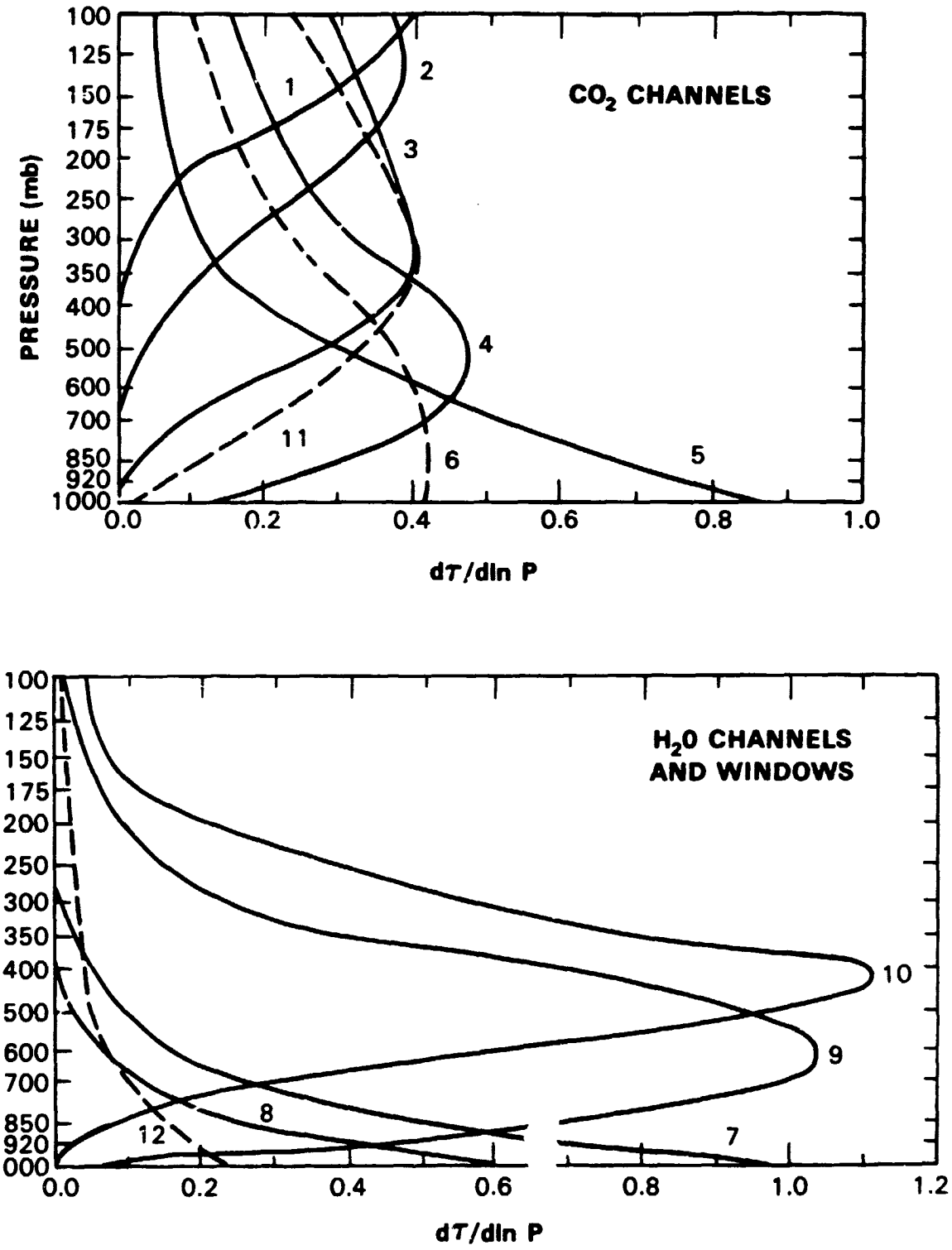

Figure 1: Standard VAS weighting functions

Figure 1 shows the weighting functions, $d\tau/d\ln P$, which were used for the construction of Table 2. These estimates are calculated for the U.S. Standard Atmosphere, using the spectral response functions listed in Appendix A. VAS transmittance functions, $\tau(\nu,P)$, are computed for each channel at wavenumber ν, down to pressure level P. The transmittances are calculated using line-by-line absorption coefficients for CO_2, N_2, N_2O, NO, CH_4, O_2 and H_2O (McClatchey et al., 1973), and using molecular continuum absoption cross sections for H_2O, N_2 and CO_2 (Burch et al., 1970-1; Roberts, 1976).

The temperature sounding channels are plotted separately from the water vapor and window channels in Figure 1, and the shortwave channels are indicated with dashed lines. The redundancy between the longwave and shortwave channels was designed for the detection of cloud contamination, by exploiting the differential sensitivity of the Planck function to cloud top temperature. The sharp peaks of the upper air moisture channels in Figure 1 are due to the exponential distribution of water vapor in the U.S. Standard Atmosphere. In reality, the vertical structure of the water vapor weighting functions is not readily predictable or retrievable because they represent the radiance accumulation from the top few millimeters of the total water burden. On the other hand, VAS images in these channels provide high resolution information about the horizontal distribution of thick layers of water vapor. Figure 1 also shows that the lower troposphere (600 to 1000 mb) is not well resolved by any one of the VAS channels. The radiation from the lower troposphere is mixed with both surface and mid-tropospheric contributions in all the key VAS channels (5, 6, 7, 8 and 12), and the shortwave infrared window (channel 12 at 3.9 μm) is affected by reflected sunlight. No VAS water vapor channel has a peak response in the lower troposphere, although the best low-level temperature sounding channel (5 at 13.3 μm) is also sensitive to low-level water vapor. Simulat ' retrievals indicate that VAS soundings will suffer from ambiguities about the state of the lower atmosphere (Chesters et al., 1982). Actual VAS soundings confirm these expectations, and demonstrate the value of conventional surface data as an aid to resolving the lower levels (Lee et al., 1983).

2.3 VAS PRELAUNCH SPECIFICATIONS

TABLE 3

Specifications for the VAS channels

VAS Ch.	SFOV RMS	Sample Noise	Calibration Errors Absolute, Relative		Typical Scene Mean ± Dev.	
Brightness temperature units (T*, Kelvin)						
1	0.3	5.3	1.5	0.5	216.	10.
2	0.3	2.2	1.5	0.5	218.	9.
3	0.3	1.8	1.5	0.5	226.	7.
4	0.2	1.2	1.5	0.5	245.	9.
5	0.2	1.0	1.5	0.5	274.	15.
6	0.1	1.6	1.5	0.5	274.	17.
7	0.2	1.0	1.5	0.5	289.	19.
8	0.2	0.1	1.5	0.5	295.	21.
9	0.4	3.4	1.5	0.5	257.	10.
10	0.5	1.6	1.5	0.5	242.	7.
11	0.3	6.7	1.5	0.5	244.	11.
12	0.1	0.8	1.5	0.5	296.	22.
Radiance units (R, erg/etc.)						
1	0.25	4.9	1.3	0.4	40.	9.
2	0.25	2.0	1.3	0.4	42.	8.
3	0.25	1.8	1.5	0.5	48.	7.
4	0.25	1.4	1.7	0.6	66.	11.
5	0.25	1.4	2.2	0.7	100.	23.
6	0.004	0.057	0.077	0.025	1.2	0.8
7	0.25	1.4	2.5	0.8	117.	30.
8	0.25	0.16	2.5	0.8	110.	36.
9	0.15	1.3	0.6	0.2	14.	4.
10	0.10	0.33	0.3	0.1	5.7	1.5
11	0.004	0.066	0.020	0.006	0.23	0.14
12	0.004	0.020	0.054	0.018	0.84	0.79

Table 3 lists the prelaunch sounding specifications for VAS performance (Montgomery and Endres, 1977). The sounding-field-of-view (SFOV) requirements for absolute RMS errors are based upon the principle that the input to a remote sensing algorithm must be more accurate than the output. For example, ±0.2 K input errors in brightness can produce ±2.0°C output errors in atmospheric temperature after differences are taken among a dozen channels. The sounding error budget was drafted

with the expectation of spatial averaging to 30x30 km² horizontal resolution at nadir (150x150 km² for VAS channel 1). The single-sample noise values are based upon the anticipated detector-amplifier noise and filter bandwidths[1]. The noise specifications apply to the large detectors. The single-sample noise was expected to be twice as large for the small detectors, so that horizontal averaging should produce the same signal-to-noise for the same spatial resolution. Nominal calibration requirements are ±1.5 K absolute and ±0.5 K relative brightness temperature accuracy. Some of the faint channels (1, 9 and 11) have single-sample noise values which are much larger than the SFOV requirements, so that these bands are expected to require a large spin budget. While the shortwave channels appear to be relatively noisy, they can provide very large contrast over the earth, as can be seen by comparing the mean and RMS deviation from the mean of the Earth's brightness listed in the last two columns of Table 3 for VAS channels 6, 11 and 12. The brightness difference between shortwave and longwave channels with similar weighting functions (see Figure 1) is expected to aid in the detection of clouds.

---

[1] The single-sample noise estimates listed in Table 3 are 10% to 50% smaller than the official engineering specifications (compare Montgomery and Endres, 1977, page 10, to Malinowski and Ruiz, 1980, page 66 in Appendix A). The NEΔR values used by SBRC are: 10.4, 3.5, 3.0, 2.2, 2.1, 0.063, 1.9, 0.30, 1.8, 0.48, 0.073 and 0.022 erg/etc. for VAS channels 1 through 12, respectively. This report uses the more stringent values as a benchmark because prelaunch planning was based upon them. The measured VAS noise was less than either set of specifications.

Section 3

THE VAS DATA CHAIN

3.1 RADIOMETRY PERFORMED BY THE VAS GROUND SYSTEM

VAS radiometric calibration is complicated by the lack of external references (except for outer space), and by the glow of the foreoptics. Many calibration steps are performed within the long chain of computers between the satellite and the user. This section is a detailed review of important functions in the VAS data chain and of some of the problems which were experienced during the VAS Demonstration. A summary of the impact of the ground system upon the usefulness of VAS data is provided in the section which appraises the radiometric performance.

VAS calibration techniques were developed by Santa Barbara Research Center (SBRC) (Malinowski and Ruiz, 1980), to meet the requirements of the operational subcontractor, the Space Science and Engineering Center at the University of Wisconsin (SSEC or UW) (Menzel, 1980). The Westinghouse Corporation developed the ground systems which handle the VAS data stream and carry out the calibration calculations (Anon., 1978a, 1978b, 1979a, 1979b, 1979c, 1979d, 1979e and 1980).

3.2 REVIEW OF THE VAS DATA CHAIN

Goddard Space Flight Center (GSFC) maintains a computer system capable of utilizing VAS data, known as the VAS Processor (VASP). Before the VASP receives the data, it is processed by three other computers:

- The hardware on board the GOES satellite performs the initial sampling and calibration observations.
- The computer located at the NOAA ground station is known as the Synchronizer/Data Buffer (S/DB). The S/DB performs radiance corrections, line-by-line calibration determinations, radiance resampling of every line, and data stretching functions.
- The GSFC front end computer is called the VAS PreProcessor (VASPP). The VASPP performs archiving, data unpacking, zero point subtraction, dwell averaging, and line-by-line documentation functions.

The VASP itself reformats the radiance data either to make images or to compute soundings from carefully averaged SFOVs. Calibration problems are normally undetected until they hit the VASP.

3.2.1 Calibration on GOES

Each scanline is calibrated by viewing an internal calibration target (nominally at 320 K) and outer space (nominally at 3 K, but effectively at zero radiance for VAS noise levels). Because the hot calibration target is located between the telescope and the infrared detectors, the calibration algorithm must correct for the radiation received from the VAS foreoptics, whose component temperatures are monitored to $\pm 0.1^{\circ}C$ by the GOES system. The raw voltage measured from an infrared detector is converted into a 10-bit "count" for each sample on the scanline. The positive bias and the leeway allowed in this conversion leaves little more than 8 significant bits of useful signal (approximately $2^{-8}=0.4\%$ truncation error). A slow change in the detector bias during a scanline is termed "droop", since a steady discharge in the electronics will appear as a downward drift in the zero level radiance.

The sampling process is controlled by the S/DB which continually monitors the location of the Sun and estimates the relative position of the Earth relative to the GOES spacecraft. The aim is to commence sampling, commence broadcasting, halt broadcasting and halt sampling so that the Earth appears centered on the scanline. Feedback from the ground is accomplished by sending "pointing" offsets for the commencement times in order to truely center the Earth.

An infrared detector is sampled every $8(10^{-6})$ sec, which occurs more frequently than the detector footprint can move its own width. A low-pass 5-pole Bessel filter and a DC-restore filter are applied to the

stream of infrared samples. Consequently, this over-sampled data stream has a time constant which reduces the single sample noise but somewhat averages the successive samples (Menzel, 1980). The correlation coefficient between successive samples is 40% to 60%.

3.2.2 Calibration in the S/DB

The 2-point (3 K and 320 K) calibration curve is determined at the S/DB, and the 10-bit counts are converted to positive (i.e. still offset) values proportional to radiance. The proportionality factor for each scanline is passed as a single number representing the "binary point" position for the 10-bit samples.

The raw radiances are corrected at the S/DB for the glowing foreoptics with a 8-coefficient regression scheme, using temperature values from thermistors attached to the VAS instrument. The residual errors during prelaunch bench tests did meet specifications, with errors dominated by unexplained biases (Menzel, 1980).

The S/DB redefines the zero level values by checking both ends of each scanline, choosing the end with the smallest mean value in order to avoid confusion by some bright object, such as the moon or stars. The S/DB edits out the highest and lowest values from 34 samples at the each end of the scanline, leaving 32 samples to redefine a zero level.

The S/DB also resamples every scanline with a 3-point Largangian interpolation formula in order to correct for asynchronous sampling, startup jitter and spin rate variations. Otherwise, jitter in the VAS sampling clock would produce irregular east-west shifts in each line resulting in images of the earth with a ragged-looking limb. Likewise, drifts in the actual spin rate of the GOES satellite (nominally 100 revolutions per minute) would change the apparent angular width of the earth. The S/DB interpolates the original scanline in order to produce 3822 samples of apparently constant angular spacing.

3.2.3 Calibration in the VASPP

At the VASPP, the 10-bit values are unpacked into 16-bit integer words, the offset is removed, and dwell averaging over the "spin budget" of each channel is performed (this is called the "DSA" mode in the VASPP). The removal of the offset produces some negative radiances, observable in the noise when viewing outer space. The user can also acquire unaveraged dwell sounding (called the "DSU" mode) radiances from the VASPP, so that problems with the spin-by-spin data processing can be diagnosed.

3.2.4 Calibration in the VASP

At the VASP, the 16-bit integer radiance counts are converted into 32-bit floating point radiances, using the "binary point scale factor", F, for each scanline. In FORTRAN notation, RAD=KOUNT*2**(F-15). The VASP user can further average lines and/or pixels together into larger, less noisy SFOVs. The VASP can also re-interleave the samples, channels, lines and documentation into datasets more conveniently organized for sounding or for imaging.

3.2.5 "Transparent" VAS Mode (TVM) Data

VAS data acquisition was not always permitted during the VAS Demonstration because VISSR mode operations preclude the VAS mode. NOAA uses GOES-5 as GOES-EAST and GOES-5 and -6 as GOES-WEST, especially during severe storms. The AVE/VAS experiment operated only on weekends in order to minimize the impact upon the weekday VISSR schedule. During the VAS Demonstration, a "Transparent" (to the VISSR users) VAS Mode (TVM) was devised. The additional independent detectors on the VAS instrument can provide simultaneous VISSR (visible and 11 μm) and VAS (2 additional infrared channels) data streams during the operational full disk imaging (first 20 minute of each half hour). In the non-imaging intervals (last 10 minutes of each half hour) some VAS dwell sounding can also be accomplished. The TVM innovation alleviated the demand for daily VAS data for research and development.

3.3 PROBLEMS ON THE VAS DATA CHAIN

This section describes some of the problems encountered during the VAS Demonstration. These serve as a checklist for diagnosing most of the irregularities which a sounding scientist can face in processing VAS data. The frequency of occurance is quite irregular, improving whenever the VAS system is used routinely.

3.3.1 Bit Errors during Data Transmission

The ground processing system was designed to provide a bit error rate of less than 1 per 10^6. Bit errors in the redundant line-by-line documentation are detected and corrected, but errors in the radiances are not. The most significant bit errors are noticeable as isolated extreme values in the radiances.

3.3.2 Predicted/Actual Header Mismatches

The VAS data chain is a "bucket brigade" -- the computers are triggered by the arrival of each scanline. The chain does not sense a dropped record because some links expect the data to arrive in a predetermined order. Consequently, a dropped record causes problems such as misapplied calibration, dwell averaging of unlike channels and discontinuous images. The VASPP or VASP can diagnose a missing record after a frame has completed by examining the line-by-line documentation of unaveraged data to verify that the predicted header values (filter, scanline and detector size) match the actual values. The most common causes for these drops are either antenna misalignments between GOES and the S/DB, or hardware errors in the computers. Antenna misalignments are corrected by NOAA operations at Wallops. Although hardware errors are normally infrequent, this problem was especially acute in the winter of 1980-1, when it was traced to corroding silver-coated leads on some of the integrated circuits in the S/DB. Since then, the leads have been solder-coated and the problem minimized. In either case, the impact of a lost record was severe enough to make the entire VAS frame useless.

3.3.3 Incomplete Frames

It is common for the last 3 to 8 scanlines in a VAS frame to be "lost" at GSFC between the VASPP and VASP. Data acquisition software in the VASP is suspected to over-anticipate the end of the frame. This shortens each frame by an unpredictable amount, and makes it impossible for the VASP to acquire a test frame which consists of a few scanlines.

3.3.4 Timing Errors

VAS data arrives at a rate of 1.75 Mbits per second (approximately 1 Mbytes per minute). This rate approaches the limits of the S/DB and VASPP so that the software can fail to clear all of the previous data before the arrival of the next scanline. The user then gets mixed errors in calibration and documentation. Such errors occur when timing-sensitive software in the S/DB or VASPP is modified but not thoroughly tested.

3.3.5 VDM Pointing

The sampling process on board the GOES satellite can begin before or stop after the detectors are actually turned on and looking at outer space. This introduces large random numbers into the first or last few values on a scanline, which can seriously affect the zero point determination for outer space and cause the calibration bias to jitter noticeably from line to line. The satellite timing is controlled by the NOAA ground station with an offset parameter called "VDM pointing", which is adjusted manually until the start and end of the scanlines are both located in outer space and both contain values near zero.

3.3.6 Satellite Mis-identification

Each VAS instrument has individually determined calibration coefficients for the glowing foreoptics. The correction factors for one VAS instrument were occasionally misapplied to another VAS instrument when the NOAA receiving station at Wallops Island reloads the system or switches between GOES-EAST and GOES-WEST. Automatic satellite identification and validation procedures were almost non-existant along the VAS data chain, so that confusion of this sort was difficult to detect. This results in radiances which are systematically miscalibrated, causing unexpected biases in the satellite retrievals.

3.3.7 Binary Truncation

VAS radiances are represented by binary values of limited precision. The initial 8 to 9 bit dynamic range used for 3 to 320 K and the subsequent arithmetic operations can noticeably truncate the data and produce "quantization noise" in the radiances. For instance, 320 K at 11 μm corresponds to 155 erg/etc.. If this is represented by a digital voltage of 2^8=256, the truncation error is then 155/256=0.6 erg/etc.. Radiometric biases due to truncation will be approximately one-half of this amount. Truncation errors are most noticeable when viewing radiometric noise against the background of outer space or when viewing the intrinsically faint upper air channels.

3.3.8 Detector-to-Detector Misregistration

The footprints of the six infrared detectors are offset from each other. Prelaunch values are used by the S/DB to register scanlines by resampling in the east-west direction. North-south offsets are not corrected. The user must make any final registration corrections. Postlaunch values have been obtained by viewing landmarks with all six infrared detectors (Chesters et al., 1984). North-south misregistration is not apparent among the infrared detectors. The east-west misregistration are comparable to the IGFOV of a large detector (0.384 mrad), so that postlaunch adjustments are necessary for optimum registration between lines from the different detectors. Postlaunch offsets were determined for all three VAS instruments (Chesters et al., 1984). The S/DB normally supplied only the prelaunch values, except for VAS-E, which was updated to postlaunch offsets in January, 1982.

3.3.9 East-West Scanline Misregistration

Figure 2 shows an example of two pairs of misregistered scanlines across the central United States, taken by VAS-E with the 11 μm window channel during the AVE/VAS Special Network Experiment (Greaves et al., 1982) at 1430 GMT on 24 April 1982. The effective east-west "pointing" of each scanline is controlled by the S/DB, which resamples all of the data in order to correct for detector offsets and for irregularities in the startup time of the sampling clock on GOES. Unfortunately, scanlines occasionally show quite noticeable (tens of samples) east-west shifts of an entire scanline. The cause of the difficulty is unknown. The impact on the cosmetic quality of images and on dwell or spatial averaging can be significant if not corrected.

Figure 3 shows a 126-sample segment of VAS-F data taken on 24 May 1983 over the partly cloudy Pacific for two dwell-mode spin scans with the same channel, detector and scanline. The east-west registration "jumps forward" for about 20 samples at one point, returns to normal, "falls back" by one sample for a while, and then returns to normal. It appears that this kind of slight misregistration occured from 8% to 50% of the time within segments of each scanline. The fault lay in the resampling hardware of the S/DB, which was corrected in September, 1983.

3.3.10 "Scattered Light"

Figure 4 presents two segments of the same scanline, in order to display the "scattered light" just beyond both limbs of the earth. Data for VAS-E is shown from the large upper longwave detector using the 11 μm filter on 4 August 1981. The east (trailing) limb shows substantially more radiance in outer space than does the west (leading) limb. This asymmetry suggests that there is an unexpectedly long time constant in the data processing chain.

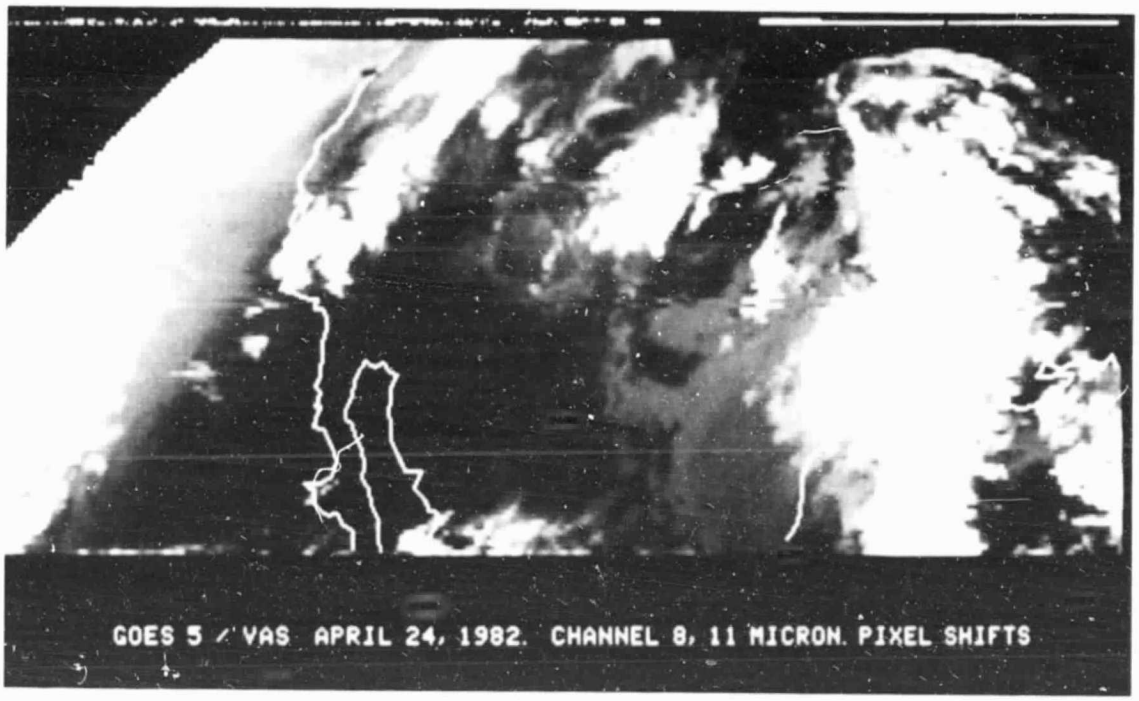

Figure 2: East-west shifts of entire VAS scanlines

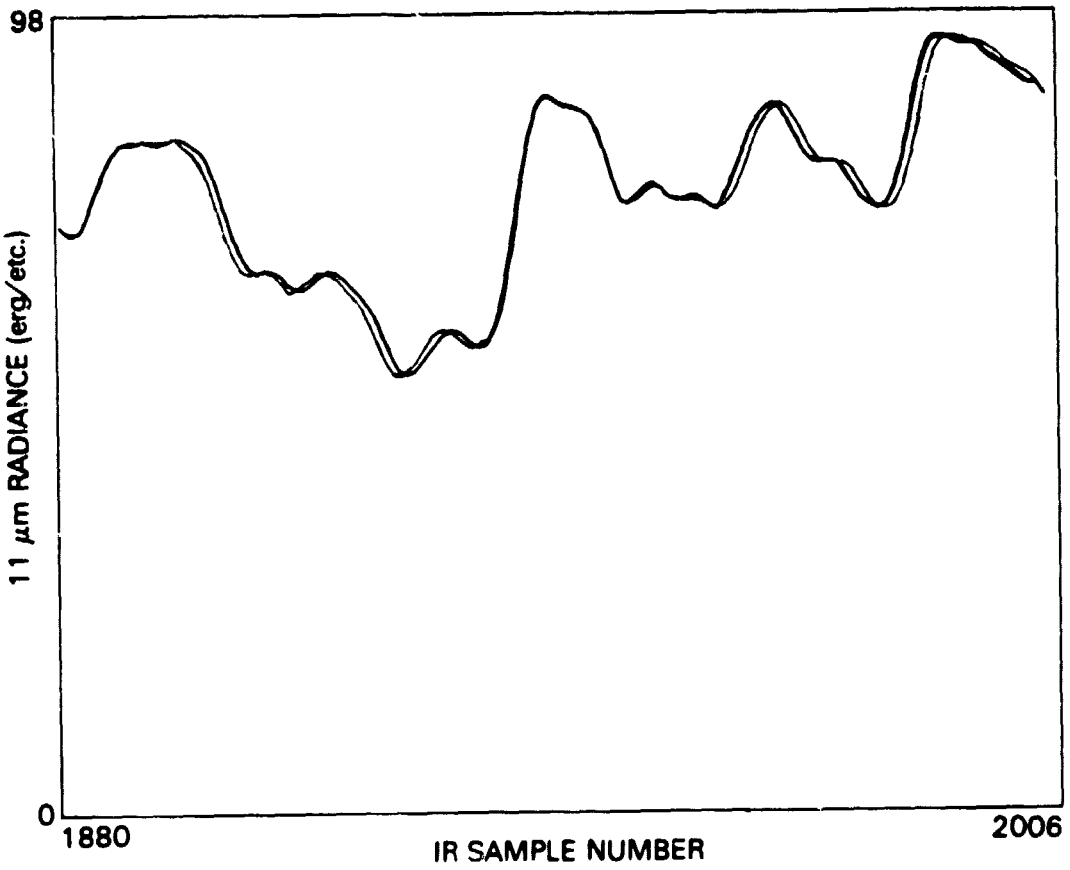

Figure 3: East-west misregistration within scanlines

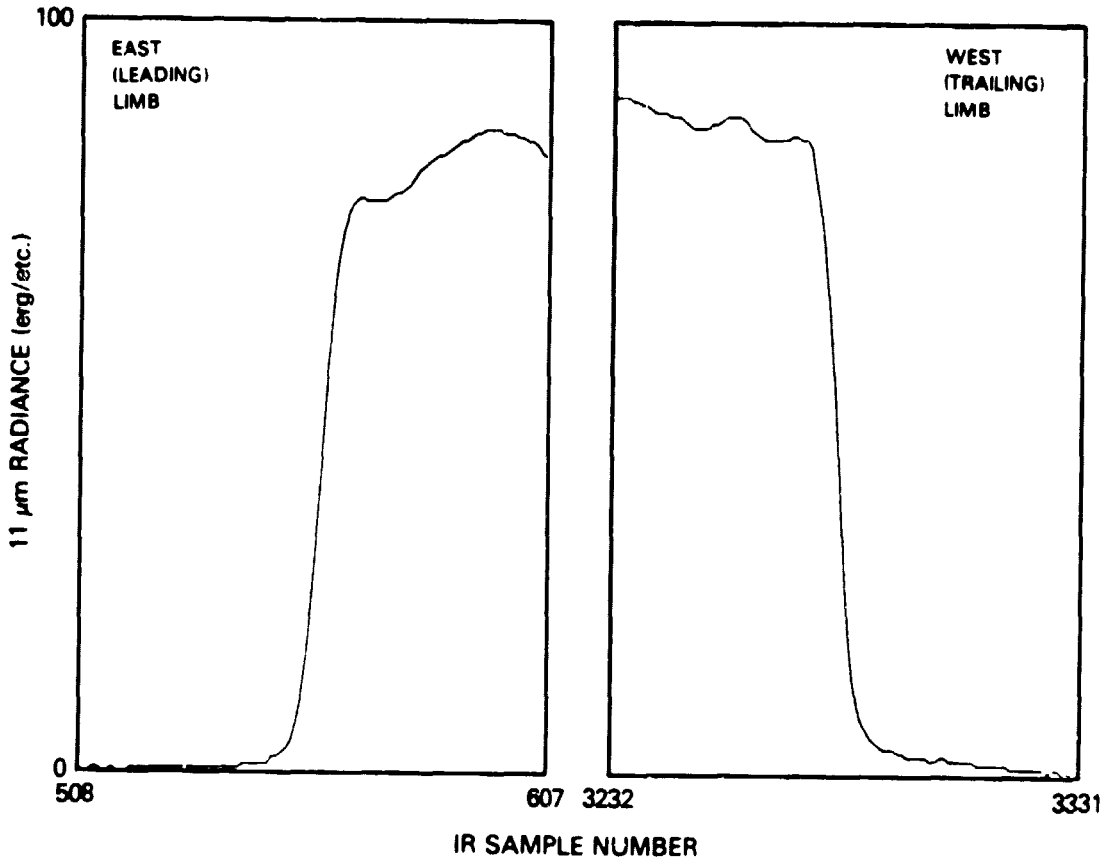

Figure 4: "Scattered light" beyond the limbs of the earth

Section 4

VAS RADIOMETRIC PERFORMANCE APPRAISAL

The VAS channels operate with detector pairs, producing an "upper" and "lower" scanline with each spin. Postlaunch performance appraisals for every filter-detector combination on GOES-4, -5 and -6 are presented in Appendix B. The following tables summarize these results with a single value for each kind of error for each channel. These tables are constructed by selecting the worst of the values measured for the upper and lower detectors on each VAS instrument, in order to be properly cautious about the useful quality of the data. On GOES-4, the upper large detectors never functioned, and the S/DB software for the small detectors was not debugged in time for their evaluation. On GOES-5, the errors in both detectors were very similar for all bands. On GOES-6, the errors are dominated by a noisy lower large longwave detector.

4.1 RADIOMETRIC NOISE AND AVERAGING FACTORS

TABLE 4

Radiance noise observed in the VAS channels

VAS Ch. No.	Specified Single-sample Noise	Standard deviation in outer space GOES-4 18 Feb 81	GOES-5 4 Aug 81	GOES-6 24 May 83
		Large detector noise (erg/etc.)		
1	4.9	4.4	2.8	2.8
2	2.0	2.6	1.5	1.8
3	1.8	1.5	1.1	1.4
4	1.4	1.4	0.9	1.2
5	1.4	1.2	0.8	0.7
6	0.057	0.031	0.023	0.021
7	1.4	0.9	0.8	0.9
8	0.16	0.2	0.2	0.3
9	1.3	1.2	0.6	0.7
10	0.33	0.3	0.2	0.2
11	0.066	0.030	0.027	0.023
12	0.020	0.008	0.007	0.009
		Small detector noise (erg/etc.)		
3	3.6	n.a.	2.5	2.4
4	2.8	n.a.	1.9	2.1
5	2.8	n.a.	1.5	1.6
7	2.8	n.a.	1.4	1.5
8	0.32	0.4	0.3	0.3
9	2.6	n.a.	1.3	1.2
10	0.67	n.a.	0.3	0.3

Table 4 compares the single-sample noise observed for the VAS channels to the prelaunch specifications. The noise was measured by taking the standard deviation of 200 successive samples from outer space. The postlaunch noise measurements are better than the design specifications, especially in the case of the shortwave window (channel 12). GOES-4 carried the noisiest VAS instrument, GOES-5 carried the quietest, and GOES-6 carried a noisy large lower longwave detector which dominates these statistics. The small detectors are less than twice as noisy as the large, making them potentially very useful for high resolution work.

TABLE 5

Space-time averaging factors for a SFOV

VAS Ch. No.	Specified SFOV Req. (erg/etc.)	(Dwell spins) x (Independent samples) GOES-4 18 Feb 81	GOES-5 4 Aug 81	GOES-6 24 May 83
		Large detector averaging factors		
1	0.25	310.	125.	125.
2	0.25	108.	36.	52.
3	0.25	36.	19.	31.
4	0.25	31.	13.	23.
5	0.25	23.	10.	13.
6	0.004	60.	33.	28.
7	0.25	13.	10.	13.
8	0.25	1.	1.	1.
9	0.15	64.	16.	22.
10	0.10	9.	4.	4.
11	0.004	56.	46.	33.
12	0.004	4.	4.	4.
		Small detector averaging factors		
3	0.25	n.a.	100.	92.
4	0.25	n.a.	58.	71.
5	0.25	n.a.	36.	41.
7	0.25	n.a.	31.	36.
8	0.25	3.	1.	1.
9	0.15	n.a.	75.	64.
10	0.10	n.a.	9.	9.

Table 5 lists estimates for the number of independent samples which each VAS channel requires to reduce the random noise values in Table 4 down to the specified sounding requirements. Because random errors decrease in proportion to the square root of the number of observations the averaging factor is $(NE\Delta R/SFOV)^2$. Noise reduction can be accomplished by both dwell and spatial averaging. Because successive scanline values are geometrically oversampled and electronically correlated, one must average 3 to 5 successive samples in order to produce 1 spatially independent observation. For instance, the averaging factor for VAS channel 1 on GOES-5 is $(2.8/0.25)^2 = 125$, which could be accomplished by combining a spin budget of 5 dwell scans with 5 independent (15 to 25 succesive) samples on each scanline from 5 adjacent scanlines. The resulting SFOV has random noise equal to the sounding requirements and has horizontal resolution of approximately 75 km. Of course, the actual error budget is larger, due to systematic

calibration errors and to horizontal inhomogeneities. Maximum horizontal resolution (16 km) could be maintained for all channels by using a spin budget equal to the averaging factors, but the time required to scan the United States would be prohibitive at the 100 rpm spin rate of the GOES satellite. In theory, one could attain the low noise levels required for sounding in 30x30 km² SFOVs (150x150 km² for VAS channel 1) with spin budgets of 50 to 70 spins per scanline (Chesters et al., 1984). In practice, dwell time was exchanged for more latitudinal coverage by giving little or no time to the noisy channels (1, 2, 6, 9 and 11). Finally, Table 5 indicates that the small detectors have averaging factors which are low enough to be potentially useful in areas of broken clouds, where individual cloud-contaminated footprints can be identified and rejected before spatial averaging.

4.2 TRUNCATION ERRORS

TABLE 6

Radiance errors due to 10-bit truncation

VAS Ch. No.	Specified NEΔR (±erg/etc.)	Half-truncation (erg/etc.) VAS-D	VAS-F	Specified SFOV (±erg/etc.)
1	4.9	0.50	0.25	0.25
2	2.0	0.50	0.25	0.25
3	1.8	0.50	0.25	0.25
4	1.4	0.50	0.13	0.25
5	1.4	0.25	0.25	0.25
6	0.057	0.008	0.008	0.004
7	1.4	0.25	0.25	0.25
8	0.16	0.25	0.13	0.25
9	1.3	0.063	0.063	0.15
10	0.33	0.063	0.032	0.10
11	0.066	0.008	0.002	0.004
12	0.020	0.002	0.002	0.004

Table 6 lists the VAS radiance truncation errors. Truncation occurs when full-range (0 to 320 K) radiances are transmitted from GOES as 10-bit integers. The narrowband upper tropospheric channels (1 to 4 and 9 to 11) are naturally faint, so that the earth's brightness only uses a few significant bits of the available dynamic range. Consequently, radiances are observed in distinctly quantized steps. The half-truncation values observed for GOES-4 in 1981 and for GOES-6 in 1983 are compared to the single-sample noise and the SFOV requirements. The truncation errors decreased during the two years between measurements due to improved data processing. The biases due to truncation errors have been reduced to the point where they are not significant for sounding purposes.

4.3 ZERO-POINT CALIBRATION ERROR

TABLE 7

VAS zero-point errors for outer space

VAS Ch. No.	Specified Single-sample Noise	<Outer space> GOES-4 18 Feb 81	GOES-5 4 Aug 81	GOES-6 24 May 83
		Large detector zero-point (erg/etc.)		
1	4.9	+0.6	+0.8	-0.3
2	2.0	+0.7	+0.5	-0.5
3	1.8	-0.1	-0.5	+0.4
4	1.4	-0.0	-0.5	+0.6
5	1.4	-0.2	-0.6	+0.6
6	0.057	+0.006	+0.008	+0.002
7	1.4	-0.2	-0.4	+0.2
8	0.16	-0.3	+0.0	+0.0
9	1.3	+0.1	-0.1	+0.1
10	0.33	+0.1	-0.0	+0.1
11	0.066	+0.003	+0.009	+0.010
12	0.020	-0.002	+0.002	-0.001
		Small detector zero-point (erg/etc.)		
3	3.6	n.a.	+0.5	+1.0
4	2.8	n.a.	+1.9	-1.4
5	2.8	n.a.	-1.2	+0.7
7	2.8	n.a.	-0.4	-0.5
8	0.32	-0.5	+0.9	-0.1
9	2.6	n.a.	+0.3	+0.3
10	0.66	n.a.	-0.2	+0.1

Table 7 lists the observed zero-point radiances for outer space from all three VAS instruments. The average value of 200 samples near the east and west ends of a scanline were computed, and the lower value is listed. There are no systematic trends in the sign of the zero-point errors, and their magnitudes are a fraction of the single-sample noise. Consequently, the low end of the calibration curve is well determined.

4.4 DROOP ALONG A VAS SCANLINE

TABLE 8

Radiance droop along a VAS scanline

VAS Ch. No.	Specified Single-sample Noise	<West space> - <East space> GOES-4 18 Feb 81	GOES-5 4 Aug 81	GOES-6 24 May 83
		Large detector droop (erg/etc.)		
1	4.9	-0.5	-0.8	-0.9
2	2.0	+1.0	+0.7	+1.1
3	1.8	+1.1	+0.7	+0.8
4	1.4	+0.4	-0.6	+1.6
5	1.4	+0.2	-0.4	+1.3
6	0.057	-0.006	+0.022	+0.004
7	1.4	-0.4	+0.3	+0.6
8	0.16	-0.2	-0.1	+0.1
9	1.3	-0.1	-0.2	+0.5
10	0.33	+0.0	-0.0	-0.3
11	0.066	+0.000	+0.018	-0.018
12	0.020	-0.002	+0.002	-0.002
		Small detector droop (erg/etc.)		
3	3.6	n.a.	-0.9	-1.0
4	2.8	n.a.	+1.1	+0.8
5	2.8	n.a.	-0.8	+1.3
7	2.8	n.a.	-1.3	+0.5
8	0.32	-0.5	-0.2	+0.0
9	2.6	n.a.	+0.5	-0.5
10	0.66	n.a.	+0.1	-0.0

Table 8 lists the difference between the average radiance values of outer space to the west and east of the earth. This procedure tests for possible "droop" in the electronic bias during a scan. Systematically positive values would indicate such a decrease in the bias during the 0.1 sec scan across the earth. The observed values for all three VAS instruments are much smaller than the single-sample noise, and have random sign. The instrument maker has done an excellent job of keeping the droop below the level of detectability.

4.5 SPIN-TO-SPIN REPRODUCABILITY

TABLE 9

Relative spin-to-spin reproducability of a scanline

VAS Ch. No.	Specified Relative Calibration	Variability among dwelled scanlines GOES-4 18 Feb 81	GOES-5 4 Aug 81	GOES-6 24 May 83
	Large detector deviation of the mean (±erg/etc.)			
1	0.4	1.2	1.7	1.3
2	0.4	1.5	0.4	0.8
3	0.5	0.5	0.5	0.7
4	0.6	0.5	0.4	0.7
5	0.7	0.5	0.3	0.8
6	0.025	0.005	0.018	0.003
7	0.8	0.4	0.2	0.2
8	0.8	0.1	0.3	0.1
9	0.2	0.5	0.2	0.5
10	0.1	0.1	0.0	0.1
11	0.006	0.006	0.006	0.004
12	0.018	0.001	0.005	0.003
	Small detector deviation of the mean (±erg/etc.)			
3	0.5	n.a.	2.8	0.6
4	0.6	n.a.	0.9	0.5
5	0.7	n.a.	0.5	0.4
7	0.8	n.a.	0.6	0.5
8	0.8	n.a.	0.1	0.1
9	0.2	n.a.	0.6	0.3
10	0.1	n.a.	0.2	0.1

Table 9 lists the observed variability among VAS scanlines. The spin-to-spin variance was calculated from data which scanned the same line across the earth 9 times in each channel. The mean radiance for 1000 central samples was taken from each spin, and the standard deviation among these 9 well-determined mean values is listed. This number measures the relative calibration error among lines prior to dwell averaging. Actually, there is no design specification for relative calibration stability from spin-to-spin. The "relative" accuracy specifications in Table 3 (i.e. ±0.5 K in T* for all VAS channels) are quoted without a specific test procedure. If we adopt the variance in the mean brightness of a scanline as the test procedure,

then Table 9 indicates that the relative calibration errors exceed the specification for the noisy narrowband channels (1, 2, 9 and 11). The observed spin-to-spin relative calibration errors are approximately one-half of the observed single-sample noise. Because these are average errors for the entire scanline, north-south spatial averaging is necessary to reduce the random noise's effect upon the line-by-line calibration errors. The relative calibration errors for such spatially averaged SFOVs appear to meet the prelaunch requirements.

In sounding applications, VAS channels 1, 2, 9 and 11 are normally given little or no time in the spin budgets. However, no systematic study has been performed to determine the information content of these channels under conditions where the upper troposphere is meteorologically interesting. For instance, sudden stratospheric warmings and tropopause folding are potentially observable mesoscale phenomena which occur in the upper atmosphere, where scientific case studies have not yet been made. These channels might be used in conjunction with ozone concentration observations from the polar orbiting satellites in order to determine low pressure structures in the upper troposphere (Gatlin, 1982). Likewise, the shortwave channels have not been systematically tested for their intended function as cloud discriminators. On the other hand, the longwave sounding channels have been tested successfully for cloud height and motion assignment (Menzel et al., 1983a), and for cloud type classification (Szejwach, 1982).

In conclusion, the relative line-to-line calibration errors make it mandatory that spatial and temporal radiance averaging be employed to attain the specified sounding accuracy. Full-resolution FOVs (16x16 km^2 at nadir) have proved useful for imaging and for those soundings which can be derived from a few of the brighter channels which probe the lower atmosphere. The small detectors should prove useful for detecting cloud contaminated FOVs before spatial averaging.

4.6 ABSOLUTE CALIBRATION ERRORS

Absolute calibration of the VAS instrument cannot be verified rigorously because there are no external standard targets available. Consequently, independent measurements must be attempted by comparing VAS radiances to nearly colocated HIRS radiances or simulated radiances at cloud-free radiosonde sites. In previous studies of GOES-4 (Menzel et al., 1981; Chesters et al., 1981) and from other data (Chesters et al., 1984), the 15 μm bands (VAS channels 2, 3 and 4) were found to exhibit a negative bias reaching 2 to 3 K with respect to both HIRS predictions and radiation transfer calculations. Consequently, sounding algorithms must be bias-resistant in order to derive soundings with the desired absolute accuracy from VAS radiances. The surface viewing bands 7, 8 and 12 are very sensitive to good navigation and time coincidence. The water vapor bands 9 and 10 are sensitive to the constancy of the water vapor concentration in each satellite's field-of-view and to inaccurate dewpoint observations by radiosonde instruments in the upper air. Therefore, terrestrial calibration tests for these bands are inconclusive.

4.7 "SCATTERED LIGHT" AND RESAMPLING ERRORS

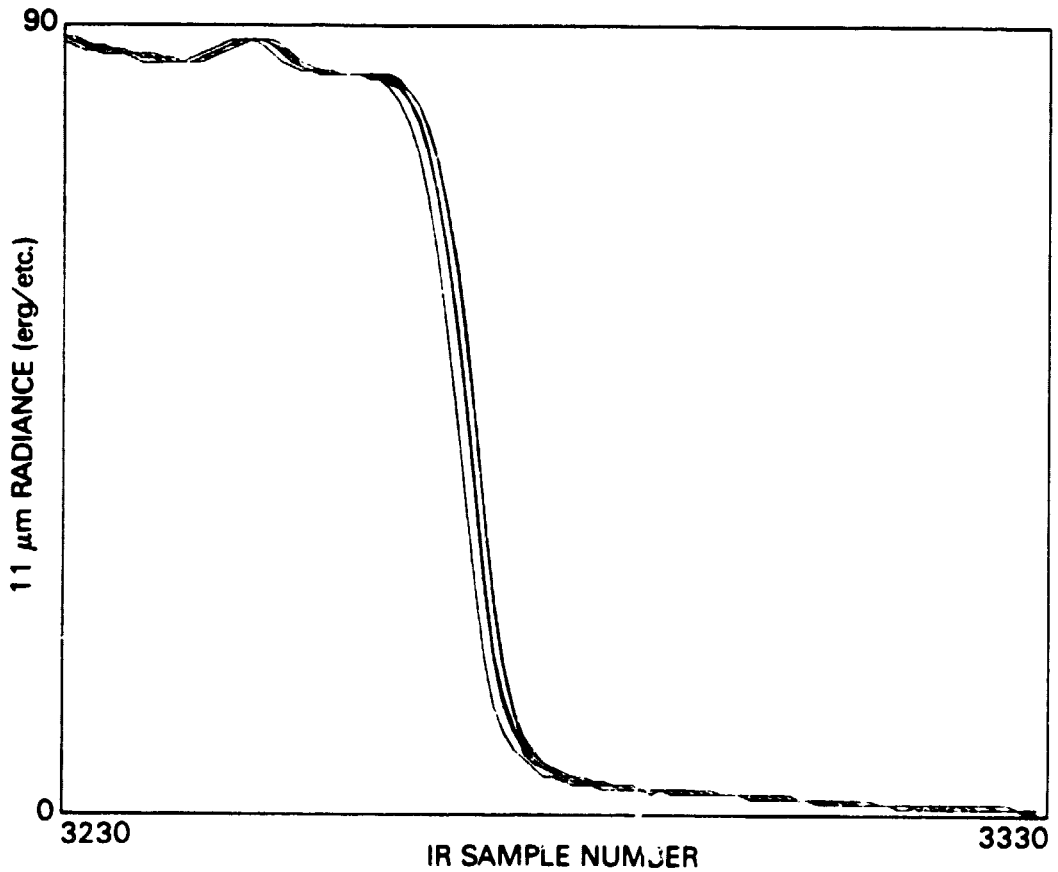

Figure 5: Repeated scans of the Earth's limb at 11 μm

Figure 5 shows a plot of 9 repeated radiance scans of the same line with the same filter and detector for 100 samples containing the east limb of the Earth. This data is for the VAS 11 μm channel on GOES-5 in August 1981. Figure 5 displays two radiometric errors which would hinder very high resolution (16x16 km^2 SFOV) sounding with VAS: "scattered light" and east-west misregistration.

The "scattered light" displayed in Figure 5 is typically 2 to 3 erg/etc. at 10 to 20 samples beyond the limb, decreasing to near 0 erg/etc. at 50 to 100 samples from the limb. "Scattered light" could be due to optical surface scattering, diffraction or electrical filter characteristics. Prelaunch measurements of the effective field-of-view indicate that 99% of the light should be received from within a circle with a radius of 0.932 mrad (approximately 15 samples). Less than 1 erg/etc. is indeed observed at 10 to 20 samples before the west limb of the earth (see Figure 4). However, the higher levels observed in Figure 5 after the east limb appear to be due to an unexpectedly long time constant. In any case, Figure 5 implies that "scattered light" contributes a few percent smoothing to the contrast within a scene. Prelaunch studies indicate that the anticipated diffraction effects are not serious for 30x30 km^2 SFOVs (Menzel, 1980).

The limb of the Earth in Figure 5 is distinctly resolved for each spin, but the east-west location varies by $\pm$1 sample. This error is not a fixed offset for the entire line, but rather it occurs irregularly within each line for lengths ranging from 10 to 50 samples (see Figure 3). Every scanline pair which has been examined contains short segments of such misregistration. Strings of systematic errors like those in Figure 5 errors are introduced 8% to 50% of the time. The radiance errors from misregistration depend upon the local horizontal gradients. Errors of only 1 erg/etc. are larger than the SFOV requirements for the VAS 11 μm window channel (see Table 3). This jitter can reduce the value both of dwell averaging and of very high resolution channel-to-channel comparisons, such as the "split window" calculations of low-level moisture (Chesters et al., 1983). The resampling in the S/DB hardware was improved in order to remove these slightly misregistered segments after September, 1983.

4.8 GROUND SYSTEM OPERATIONS

The ground system occasionally has operational difficulties which affect the usefulness of the radiances or otherwise prevent data transfer:

- Shortly after the launch of GOES-4, the S/DB computer developed sporadic problems that were traced to corroding leads on some of the chips, which were then refurbished. These problems are now rare, and taught us the importance of designing for hardware redundancy and of scheduling time for debugging.

- An entire scanline would be "dropped" in the VAS data chain due to data transmission errors. This caused dwell averaging software to incorrectly mix channels together. Such errors were detected only after data reception had been completed, and images or data headers were examined.

- Large east-west shifts of an entire scanline (by tens of samples) are sometimes observed in VAS images (see Figure 2), probably due to timing errors in the resampling at the S/DB. These are difficult to detect in dwell soundings because sounding data is temporally averaged and then used without visual quality assurance of every channel.

- Satellite-to-earth coordinate transformations were initially in error by 50 to 100 km. After corrections were made to the navigation-determination software, VAS earth-location errors met the requirements for absolute accuracy (±10 km) whenever landmark corrections were processed on a daily basis.

- Antenna misalignment between the satellite and ground system causes high bit-error rates and "lost" lines. Such problems were common at the start of an observing day.

- GOES' geosynchronous orbit causes the satellite to pass directly between the Sun and the Earth at noontime during equinox. Consequently, VAS data reception is not practical for one hour near local noon during March, April, September and October.

- NOAA's operational requirements for the GOES satellite superseded the planned observing schedule, so that less than the expected 79 days (1896 hours) of VAS data were acquired during the VAS Demonstration.

These problems were rare enough to provide the VAS Demonstration with enough experimental data to meet its basic objectives. Data reliability was good during concentrated efforts, exceeding 97% for the AVE/VAS Special Network Experiment (Greaves et al., 1982). The VAS instruments are robust enough for operational use, but the experimental ground system would require more resources to develop an equally reliable level of performance.

Section 5

SUMMARY AND DISCUSSION

The postlaunch performance of the VAS radiometer meets its prelaunch design specifications, particularly those related to image formation and noise reduction. The best VAS instrument is carried on GOES-5, currently operational as GOES-EAST. Single-sample noise is lower than expected, especially for the small longwave and large shortwave detectors. Detector-to-detector offsets are correctable to within the resolution limits of the instrument. Truncation, zero-point and droop errors are insignificant. Absolute calibration errors, estimated from HIRS and from radiation transfer calculations, indicate moderate, but stable biases. Relative calibration errors from scanline to scanline are noticeable, but meet sounding requirements for temporally (50 to 70 spins at 100 rpm) and spatially averaged (30x30 km^2) sounding fields-of-view. "Scattered light" and resampling errors somewhat reduce contrast and channel-to-channel registration for very high resolution work. The complex ground system, which also influences the net radiometric quality of VAS data, was extensively tested and improved during the VAS Demonstration. The competing demands for both VISSR and VAS mode data were alleviated by the innovation of a "Transparent" VAS Mode (TVM), which simultaneously delivers both VISSR operational data and VAS research data.

The VAS instrument is a potentially useful radiometer for mesoscale sounding operations. Image quality is very good. Soundings derived from quality controlled data meet prelaunch requirements when calculated with noise- and bias-resistant algorithms. The information from the mid- and low-level channels is better than expected. Some good results have even been obtained at 16x16 km^2 resolution, and useful work seems possible at 8x8 km^2 resolution. The information content of the faint, noisy upper air channels remains scientifically untested. While the distant geosynchronous station of the VAS instrument makes accurate radiometry difficult, the frequent and relatively stable measurements which VAS provides at fixed angle and resolution permits mesoscale measurements which were previously unavailable.

Acknowledgements: This work has been funded by the Operational Satellite Improvement Program (OSIP) and the Severe Storms Research Program (SSRP) at NASA Headquarters. The VAS Demonstration was managed at NASA/GSFC by Dr. Harry Montgomery and Mr. James Greaves. Dr. Harry Montgomery of GSFC and Mr. Paul Menzel of SSEC were principally responsible for the design, testing and improvement of VAS radiometry during the VAS Demonstration. We thank Dr. Montgomery for his aid in acquiring special test datasets and for his corrections to this independent review.

Appendix A

VAS SPECTRAL RESPONSE

TABLE 10

VAS filters: centers and halfwidths (cm^{-1})

Ch. No.	Specification ν_0	Specification $\Delta\nu$	Measurement $\langle\nu\rangle$	Measurement FWHM
1	678.7	10.	679.8	11.
2	690.6	16.	690.2	11.
3	701.6	16.	700.2	14.
4	713.6	20.	714.5	17.
5	750.	20.	750.3	18.
6	2210.	45.	2208.	45.
7	790.	20.	789.	21.
8	895.	140.	897.	146.
9	1377.2	40.	1374.9	35.
10	1487.	150.	1486.1	153.
11	2250.	40.	2253.	41.
12	2535.	140.	2541.	133.

Table 10 lists a comparison between the general filter specifications (center and halfwidth) and the prelaunch measurements (see below). All 12 VAS filters meet their spectral response specifications, with approximately triangular or trapezoidal response curves.

The following tables list the net spectral response, f(v), of the VAS filters, detectors and foreoptics as a function of wavenumber, v in cm^{-1}, for all 12 bands. These values were measured for VAS-D with large detectors, with fixed viewing angle and filter tempertures, and were interpolated to a regular wavenumber grid. The response is normalized so that f(v) has a maximum value of 0.9999. The response-weighted average wavenumber, $\langle\nu\rangle=\int\nu f(\nu)d\nu/\int f(\nu)d\nu$, is listed for each VAS channel. The actual response may vary for other instruments, detectors and operating conditions.

TABLE 11

Response for VAS channel 1, <v> = 679.786 cm^{-1}

v	f(v)	v	f(v)
667.0	.0020	689.5	.0715
667.5	.0052	690.0	.0614
668.0	.0087	690.5	.0509
668.5	.0122	691.0	.0402
669.0	.0175	691.5	.0294
669.5	.0277	692.0	.0232
670.0	.0380	692.5	.0191
670.5	.0486	693.0	.0149
671.0	.0728	693.5	.0108
671.5	.1091	694.0	.0066
672.0	.1475	694.5	.0025
672.5	.2249		
673.0	.3240		
673.5	.4265		
674.0	.5381		
674.5	.6321		
675.0	.6802		
675.5	.7111		
676.0	.7380		
676.5	.7654		
677.0	.7931		
677.5	.8300		
678.0	.8771		
678.5	.9242		
679.0	.9617		
679.5	.9841		
680.0	.9999		
680.5	.9962		
681.0	.9764		
681.5	.9334		
682.0	.8776		
682.5	.8199		
683.0	.7603		
683.5	.6987		
684.0	.6352		
684.5	.5695		
685.0	.4986		
685.5	.4257		
686.0	.3508		
686.5	.2750		
687.0	.2153		
687.5	.1798		
688.0	.1435		
688.5	.1061		
689.0	.0826		

TABLE 12

Response for VAS channel 2, $\langle v \rangle = 690.243\ cm^{-1}$

v	f(v)	v	f(v)
670.0	.0004	692.5	.9875
670.5	.0016	693.0	.9999
671.0	.0031	693.5	.9742
671.5	.0046	694.0	.9157
672.0	.0062	694.5	.8076
672.5	.0077	695.0	.6980
673.0	.0093	695.5	.5883
673.5	.0112	696.0	.4899
674.0	.0135	696.5	.4132
674.5	.0159	697.0	.3354
675.0	.0184	697.5	.2581
675.5	.0209	698.0	.1979
676.0	.0234	698.5	.1676
676.5	.0260	699.0	.1380
677.0	.0312	699.5	.1131
677.5	.0394	700.0	.0932
678.0	.0479	700.5	.0732
678.5	.0566	701.0	.0597
679.0	.0677	701.5	.0544
679.5	.0869	702.0	.0494
680.0	.1065	702.5	.0443
680.5	.1267	703.0	.0392
681.0	.1584	703.5	.0341
681.5	.2019	704.0	.0289
682.0	.2477	704.5	.0237
682.5	.2947	705.0	.0185
683.0	.3429	705.5	.0134
683.5	.3924	706.0	.0082
684.0	.4403	706.5	.0030
684.5	.4889	707.0	.0003
685.0	.5371		
685.5	.5757		
686.0	.6105		
686.5	.6460		
687.0	.6795		
687.5	.7042		
688.0	.7232		
688.5	.7425		
689.0	.7621		
689.5	.7819		
690.0	.8097		
690.5	.8459		
691.0	.8842		
691.5	.9229		
692.0	.9621		

TABLE 13

Response for VAS channel 3, $\langle v \rangle = 700.170\ cm^{-1}$

v	f(v)	v	f(v)
683.0	.0011	705.5	.9700
683.5	.0028	706.0	.8735
684.0	.0044	706.5	.7468
684.5	.0061	707.0	.6192
685.0	.0079	707.5	.4837
685.5	.0097	708.0	.3470
686.0	.0120	708.5	.2577
686.5	.0162	709.0	.2010
687.0	.0211	709.5	.1440
687.5	.0300	710.0	.0972
688.0	.0447	710.5	.0653
688.5	.0601	711.0	.0466
689.0	.0759	711.5	.0363
689.5	.1033	712.0	.0274
690.0	.1383	712.5	.0193
690.5	.1741	713.0	.0143
691.0	.2217	713.5	.0118
691.5	.2828	714.0	.0093
692.0	.3466	714.5	.0067
692.5	.4112	715.0	.0042
693.0	.4826	715.5	.0016
693.5	.5597		
694.0	.6378		
694.5	.7157		
695.0	.7799		
695.5	.8133		
696.0	.8459		
696.5	.8713		
697.0	.8879		
697.5	.9045		
698.0	.9127		
698.5	.9047		
699.0	.8966		
699.5	.8871		
700.0	.8756		
700.5	.8641		
701.0	.8525		
701.5	.8408		
702.0	.8399		
702.5	.8614		
703.0	.8940		
703.5	.9266		
704.0	.9595		
704.5	.9869		
705.0	.9999		

TABLE 14

Response for VAS channel 4, <v> = 714.452 cm^{-1}

v	f(v)	v	f(v)
694.0	.0009	716.5	.9629
694.5	.0025	717.0	.9419
695.0	.0039	717.5	.9152
695.5	.0055	718.0	.8884
696.0	.0070	718.5	.8616
696.5	.0086	719.0	.8347
697.0	.0102	719.5	.8061
697.5	.0118	720.0	.7666
698.0	.0135	720.5	.7186
698.5	.0164	721.0	.6705
699.0	.0220	721.5	.6224
699.5	.0290	722.0	.5743
700.0	.0411	722.5	.5262
700.5	.0578	723.0	.4717
701.0	.0745	723.5	.4150
701.5	.0914	724.0	.3579
702.0	.1118	724.5	.3008
702.5	.1526	725.0	.2437
703.0	.2100	725.5	.1880
703.5	.2675	726.0	.1547
704.0	.3255	726.5	.1346
704.5	.3838	727.0	.1144
705.0	.4424	727.5	.0942
705.5	.5046	728.0	.0758
706.0	.5701	728.5	.0632
706.5	.6326	729.0	.0567
707.0	.6618	729.5	.0502
707.5	.6683	730.0	.0437
708.0	.6751	730.5	.0373
708.5	.6843	731.0	.0308
709.0	.6954	731.5	.0243
709.5	.7065	732.0	.0178
710.0	.7194	732.5	.0154
710.5	.7449	733.0	.0135
711.0	.7797	733.5	.0117
711.5	.8148	734.0	.0098
712.0	.8500	734.5	.0080
712.5	.8854	735.0	.0061
713.0	.9209	735.5	.0042
713.5	.9544	736.0	.0024
714.0	.9788	736.5	.0008
714.5	.9938		
715.0	.9999		
715.5	.9917		
716.0	.9781		

TABLE 15

Response for VAS channel 5, <v> = 750.349 cm^{-1}

v	f (v)	v	f (v)	v	f (v)
728.0	.0004	750.5	.9986	773.0	.0066
728.5	.0017	751.0	.9951	773.5	.0055
729.0	.0033	751.5	.9916	774.0	.0044
729.5	.0050	752.0	.9862	774.5	.0033
730.0	.0069	752.5	.9744	775.0	.0022
730.5	.0086	753.0	.9608	775.5	.0010
731.0	.0103	753.5	.9472	776.0	.0003
731.5	.0121	754.0	.9337		
732.0	.0139	754.5	.9201		
732.5	.0197	755.0	.9043		
733.0	.0264	755.5	.8769		
733.5	.0331	756.0	.8363		
734.0	.0400	756.5	.7944		
734.5	.0468	757.0	.7446		
735.0	.0536	757.5	.6908		
735.5	.0608	758.0	.6377		
736.0	.0740	758.5	.5848		
736.5	.0982	759.0	.5318		
737.0	.1224	759.5	.4771		
737.5	.1464	760.0	.4198		
738.0	.1706	760.5	.3625		
738.5	.2125	761.0	.3052		
739.0	.2546	761.5	.2600		
739.5	.2963	762.0	.2197		
740.0	.3380	762.5	.1806		
740.5	.3794	763.0	.1477		
741.0	.4271	763.5	.1251		
741.5	.4899	764.0	.1091		
742.0	.5654	764.5	.0930		
742.5	.6409	765.0	.0768		
743.0	.7162	765.5	.0644		
743.5	.7914	766.0	.0564		
744.0	.8619	766.5	.0503		
744.5	.8874	767.0	.0441		
745.0	.9081	767.5	.0379		
745.5	.9287	768.0	.0316		
746.0	.9494	768.5	.0253		
746.5	.9645	769.0	.0189		
747.0	.9720	769.5	.0150		
747.5	.9770	770.0	.0134		
748.0	.9820	770.5	.0123		
748.5	.9870	771.0	.0111		
749.0	.9920	771.5	.0100		
749.5	.9970	772.0	.0089		
750.0	.9999	772.5	.0078		

TABLE 16

Response for VAS channel 6, <v> = 2208.067 cm^{-1}

v	f(v)	v	f(v)
2158.0	.0018	2248.0	.0253
2160.0	.0085	2250.0	.0195
2162.0	.0101	2252.0	.0136
2164.0	.0145	2254.0	.0117
2166.0	.0226	2256.0	.0104
2168.0	.0322	2258.0	.0072
2170.0	.0425		
2172.0	.0535		
2174.0	.0657		
2176.0	.0963		
2178.0	.1375		
2180.0	.1983		
2182.0	.2794		
2184.0	.3726		
2186.0	.4664		
2188.0	.5748		
2190.0	.7088		
2192.0	.8438		
2194.0	.9398		
2196.0	.9856		
2198.0	.9999		
2200.0	.9983		
2202.0	.9968		
2204.0	.9951		
2206.0	.9931		
2208.0	.9883		
2210.0	.9762		
2212.0	.9643		
2214.0	.9526		
2216.0	.9447		
2218.0	.9395		
2220.0	.9343		
2222.0	.9292		
2224.0	.8890		
2226.0	.7939		
2228.0	.6703		
2230.0	.5433		
2232.0	.4105		
2234.0	.2702		
2236.0	.1763		
2238.0	.1174		
2240.0	.0797		
2242.0	.0601		
2244.0	.0419		
2246.0	.0315		

TABLE 17

Response for VAS channel 7, <v> = 789.239 cm^{-1}

v	f(v)	v	f(v)	v	f(v)
761.5	.0002	784.0	.6634	806.5	.0664
762.0	.0009	784.5	.6697	807.0	.0531
762.5	.0019	785.0	.6762	807.5	.0424
763.0	.0029	785.5	.6831	808.0	.0350
763.5	.0039	786.0	.6973	808.5	.0301
764.0	.0048	786.5	.7122	809.0	.0254
764.5	.0059	787.0	.7270	809.5	.0207
765.0	.0069	787.5	.7437	810.0	.0162
765.5	.0079	788.0	.7686	810.5	.0127
766.0	.0089	788.5	.7951	811.0	.0116
766.5	.0100	789.0	.8217	811.5	.0105
767.0	.0111	789.5	.8482	812.0	.0094
767.5	.0121	790.0	.8747	812.5	.0084
768.0	.0132	790.5	.9011	813.0	.0073
768.5	.0171	791.0	.9275	813.5	.0063
769.0	.0222	791.5	.9538	814.0	.0052
769.5	.0295	792.0	.9802	814.5	.0041
770.0	.0394	792.5	.9999	815.0	.0031
770.5	.0512	793.0	.9955	815.5	.0020
771.0	.0630	793.5	.9768	816.0	.0010
771.5	.0747	794.0	.9549	816.5	.0002
772.0	.0865	794.5	.9213		
772.5	.0982	795.0	.8741		
773.0	.1170	795.5	.8269		
773.5	.1483	796.0	.7799		
774.0	.1866	796.5	.7330		
774.5	.2249	797.0	.6862		
775.0	.2631	797.5	.6394		
775.5	.3013	798.0	.5929		
776.0	.3396	798.5	.5463		
776.5	.3778	799.0	.5045		
777.0	.4160	799.5	.4683		
777.5	.4542	800.0	.4367		
778.0	.4921	800.5	.4049		
778.5	.5220	801.0	.3733		
779.0	.5459	801.5	.3417		
779.5	.5699	802.0	.3102		
780.0	.5939	802.5	.2789		
780.5	.6141	803.0	.2477		
781.0	.6248	803.5	.2165		
781.5	.6315	804.0	.1855		
782.0	.6379	804.5	.1546		
782.5	.6443	805.0	.1239		
783.0	.6507	805.5	.0988		
783.5	.6570	806.0	.0798		

TABLE 18

Response for VAS channel 8, <v> = 897.398 cm^{-1}

v	f(v)	v	f(v)	v	f(v)	v	f(v)	v	f(v)
790.0	.0001	835.0	.5843	880.0	.9941	925.0	.8493	970.0	.4336
791.0	.0007	836.0	.6006	881.0	.9951	926.0	.8458	971.0	.4045
792.0	.0015	837.0	.6169	882.0	.9961	927.0	.8422	972.0	.3754
793.0	.0023	838.0	.6332	883.0	.9971	928.0	.8386	973.0	.3466
794.0	.0031	839.0	.6495	884.0	.9980	929.0	.8350	974.0	.3180
795.0	.0039	840.0	.6658	885.0	.9989	930.0	.8315	975.0	.2895
796.0	.0046	841.0	.6815	886.0	.9999	931.0	.8279	976.0	.2613
797.0	.0053	842.0	.6968	887.0	.9982	932.0	.8246	977.0	.2332
798.0	.0061	843.0	.7122	888.0	.9938	933.0	.8257	978.0	.2053
799.0	.0069	844.0	.7275	889.0	.9895	934.0	.8270	979.0	.1776
800.0	.0076	845.0	.7428	890.0	.9851	935.0	.8283	980.0	.1500
801.0	.0084	846.0	.7580	891.0	.9808	936.0	.8296	981.0	.1227
802.0	.0091	847.0	.7732	892.0	.9766	937.0	.8309	982.0	.1032
803.0	.0098	848.0	.7887	893.0	.9723	938.0	.8321	983.0	.0897
804.0	.0105	849.0	.8045	894.0	.9679	939.0	.8335	984.0	.0769
805.0	.0113	850.0	.8202	895.0	.9637	940.0	.8347	985.0	.0641
806.0	.0120	851.0	.8359	896.0	.9594	941.0	.8360	986.0	.0545
807.0	.0137	852.0	.8516	897.0	.9552	942.0	.8372	987.0	.0503
808.0	.0258	853.0	.8673	898.0	.9510	943.0	.8385	988.0	.0473
809.0	.0389	854.0	.8829	899.0	.9468	944.0	.8398	989.0	.0445
810.0	.0519	855.0	.8986	900.0	.9426	945.0	.8410	990.0	.0415
811.0	.0648	856.0	.9143	901.0	.9384	946.0	.8414	991.0	.0385
812.0	.0776	857.0	.9300	902.0	.9342	947.0	.8394	992.0	.0356
813.0	.0968	858.0	.9456	903.0	.9301	948.0	.8372	993.0	.0327
814.0	.1405	859.0	.9599	904.0	.9259	949.0	.8349	994.0	.0298
815.0	.1841	860.0	.9621	905.0	.9218	950.0	.8328	995.0	.0269
816.0	.2273	861.0	.9631	906.0	.9177	951.0	.8306	996.0	.0241
817.0	.2703	862.0	.9640	907.0	.9136	952.0	.8284	997.0	.0212
818.0	.3129	863.0	.9680	908.0	.9095	953.0	.8253	998.0	.0185
819.0	.3553	864.0	.9721	909.0	.9054	954.0	.8217	999.0	.0157
820.0	.3973	865.0	.9762	910.0	.9022	955.0	.8180	1000.0	.0130
821.0	.4390	866.0	.9803	911.0	.8992	956.0	.8144	1001.0	.0103
822.0	.4804	867.0	.9843	912.0	.8961	957.0	.8109	1002.0	.0094
823.0	.5215	868.0	.9883	913.0	.8931	958.0	.8073	1003.0	.0085
824.0	.5540	869.0	.9921	914.0	.8896	959.0	.7984	1004.0	.0076
825.0	.5521	870.0	.9937	915.0	.8858	960.0	.7688	1005.0	.0067
826.0	.5419	871.0	.9922	916.0	.8821	961.0	.7341	1006.0	.0058
827.0	.5315	872.0	.9908	917.0	.8785	962.0	.6995	1007.0	.0049
828.0	.5210	873.0	.9893	918.0	.8748	963.0	.6653	1008.0	.0041
829.0	.5106	874.0	.9881	919.0	.8711	964.0	.6312	1009.0	.0032
830.0	.5123	875.0	.9890	920.0	.8674	965.0	.5973	1010.0	.0024
831.0	.5259	876.0	.9901	921.0	.8639	966.0	.5637	1011.0	.0015
832.0	.5394	877.0	.9911	922.0	.8602	967.0	.5303	1012.0	.0006
833.0	.5527	878.0	.9921	923.0	.8566	968.0	.4970	1013.0	.0001
834.0	.5680	879.0	.9932	924.0	.8529	969.0	.4641		

TABLE 19

Response for VAS channel 9, <v> = 1374.872 cm^{-1}

v	f(v)	v	f(v)
1323.0	.0010	1413.0	.0320
1325.0	.0038	1415.0	.0253
1327.0	.0065	1417.0	.0188
1329.0	.0093	1419.0	.0132
1331.0	.0121	1421.0	.0096
1333.0	.0169	1423.0	.0060
1335.0	.0240	1425.0	.0024
1337.0	.0315		
1339.0	.0390		
1341.0	.0465		
1343.0	.0539		
1345.0	.0614		
1347 0	.0743		
1349.0	.1106		
1351.0	.1575		
1353.0	.2631		
1355.0	.3852		
1357.0	.5153		
1359.0	.6984		
1361.0	.8319		
1363.0	.8462		
1365.0	.8316		
1367.0	.8363		
1369.0	.8671		
1371.0	.8998		
1373.0	.9324		
1375.0	.9650		
1377.0	.9878		
1379.0	.9999		
1381.0	.9871		
1383.0	.9702		
1385.0	.9286		
1387.0	.8639		
1389.0	.7272		
1391.0	.5872		
1393.0	.4542		
1395.0	.3326		
1397.0	.2206		
1399.0	.1577		
1401.0	.1152		
1403.0	.0817		
1405.0	.0672		
1407.0	.0540		
1409.0	.0451		
1411.0	.0385		

TABLE 20

Response for VAS channel 10, <v> = 1486.123 cm^{-1}

v	f(v)	v	f(v)	v	f(v)
1376.0	.0003	1466.0	.9743	1556.0	.8730
1378.0	.0017	1468.0	.9723	1558.0	.8761
1380.0	.0032	1470.0	.9703	1560.0	.8209
1382.0	.0048	1472.0	.9683	1562.0	.6577
1384.0	.0063	1474.0	.9663	1564.0	.5044
1386.0	.0079	1476.0	.9642	1566.0	.3729
1388.0	.0094	1478.0	.9566	1568.0	.2570
1390.0	.0109	1480.0	.9405	1570.0	.1455
1392.0	.0136	1482.0	.9214	1572.0	.0956
1394.0	.0248	1484.0	.9025	1574.0	.0734
1396.0	.0406	1486.0	.8837	1576.0	.0566
1398.0	.0564	1488.0	.8648	1578.0	.0407
1400.0	.0722	1490.0	.8462	1580.0	.0267
1402.0	.1350	1492.0	.8501	1582.0	.0144
1404.0	.2193	1494.0	.8618	1584.0	.0113
1406.0	.3046	1496.0	.8749	1586.0	.0098
1408.0	.3898	1498.0	.8879	1588.0	.0064
1410.0	.4751	1500.0	.9009		
1412.0	.5603	1502.0	.9137		
1414.0	.6454	1504.0	.9260		
1416.0	.7136	1506.0	.9341		
1418.0	.7492	1508.0	.9168		
1420.0	.7770	1510.0	.8993		
1422.0	.8049	1512.0	.8818		
1424.0	.8327	1514.0	.8645		
1426.0	.8604	1516.0	.8472		
1428.0	.8882	1518.0	.8301		
1430.0	.9147	1520.0	.8130		
1432.0	.9407	1522.0	.7961		
1434.0	.9665	1524.0	.8011		
1436.0	.9913	1526.0	.8135		
1438.0	.9999	1528.0	.8274		
1440.0	.9984	1530.0	.8412		
1442.0	.9970	1532.0	.8549		
1444.0	.9955	1534.0	.8686		
1446.0	.9941	1536.0	.8821		
1448.0	.9926	1538.0	.8956		
1450.0	.9910	1540.0	.9000		
1452.0	.9889	1542.0	.8925		
1454.0	.9868	1544.0	.8782		
1456.0	.9847	1546.0	.8639		
1458.0	.9826	1548.0	.8496		
1460.0	.9806	1550.0	.8352		
1462.0	.9785	1552.0	.8423		
1464.0	.9764	1554.0	.8569		

TABLE 21

Response for VAS channel 11, <v> = 2252.567 cm^{-1}

v	f(v)	v	f(v)
2207.0	.0033	2297.0	.0080
2209.0	.0064	2299.0	.0056
2211.0	.0095	2301.0	.0033
2213.0	.0148	2303.0	.0012
2215.0	.0255		
2217.0	.0352		
2219.0	.0475		
2221.0	.0716		
2223.0	.1085		
2225.0	.1591		
2227.0	.2344		
2229.0	.3312		
2231.0	.4303		
2233.0	.5535		
2235.0	.7091		
2237.0	.8662		
2239.0	.9253		
2241.0	.9542		
2243.0	.9715		
2245.0	.9860		
2247.0	.9919		
2249.0	.9972		
2251.0	.9999		
2253.0	.9984		
2255.0	.9926		
2257.0	.9927		
2259.0	.9943		
2261.0	.9934		
2263.0	.9848		
2265.0	.9622		
2267.0	.8911		
2269.0	.7708		
2271.0	.6287		
2273.0	.4897		
2275.0	.3874		
2277.0	.2859		
2279.0	.1945		
2281.0	.1229		
2283.0	.0865		
2285.0	.0592		
2287.0	.0436		
2289.0	.0343		
2291.0	.0251		
2293.0	.0159		
2295.0	.0109		

TABLE 22

Response for VAS channel 12, <v> = 2541.063 cm^{-1}

v	f(v)	v	f(v)	v	f(v)	v	f(v)
2396.0	.0001	2486.0	.7043	2576.0	.9898	2666.0	.0021
2398.0	.0002	2488.0	.7205	2578.0	.9835	2668.0	.0014
2400.0	.0006	2490.0	.7368	2580.0	.9700	2670.0	.0007
2402.0	.0011	2492.0	.7532	2582.0	.9566	2672.0	.0003
2404.0	.0015	2494.0	.7697	2584.0	.9431		
2406.0	.0019	2496.0	.7863	2586.0	.9297		
2408.0	.0024	2498.0	.7992	2588.0	.9164		
2410.0	.0029	2500.0	.8091	2590.0	.9031		
2412.0	.0034	2502.0	.8180	2592.0	.8721		
2414.0	.0038	2504.0	.8270	2594.0	.8321		
2416.0	.0043	2506.0	.8360	2596.0	.7751		
2418.0	.0047	2508.0	.8450	2598.0	.7180		
2420.0	.0052	2510.0	.8540	2600.0	.6610		
2422.0	.0057	2512.0	.8631	2602.0	.6042		
2424.0	.0061	2514.0	.8721	2604.0	.5476		
2426.0	.0067	2516.0	.8812	2606.0	.4913		
2428.0	.0072	2518.0	.8903	2608.0	.4351		
2430.0	.0077	2520.0	.8994	2610.0	.3791		
2432.0	.0081	2522.0	.9086	2612.0	.3233		
2434.0	.0086	2524.0	.9177	2614.0	.2676		
2436.0	.0091	2526.0	.9269	2616.0	.2122		
2438.0	.0101	2528.0	.9361	2618.0	.1592		
2440.0	.0146	2530.0	.9454	2620.0	.1273		
2442.0	.0225	2532.0	.9546	2622.0	.1040		
2444.0	.0305	2534.0	.9639	2624.0	.0948		
2446.0	.0385	2536.0	.9717	2626.0	.0856		
2448.0	.0466	2538.0	.9784	2628.0	.0765		
2450.0	.0547	2540.0	.9803	2630.0	.0674		
2452.0	.0629	2542.0	.9820	2632.0	.0583		
2454.0	.0713	2544.0	.9836	2634.0	.0491		
2456.0	.1164	2546.0	.9852	2636.0	.0400		
2458.0	.1617	2548.0	.9869	2638.0	.0309		
2460.0	.2073	2550.0	.9885	2640.0	.0219		
2462.0	.2534	2552.0	.9901	2642.0	.0130		
2464.0	.2996	2554.0	.9918	2644.0	.0113		
2466.0	.3460	2556.0	.9934	2646.0	.0098		
2468.0	.3928	2558.0	.9950	2648.0	.0090		
2470.0	.4394	2560.0	.9966	2650.0	.0082		
2472.0	.4856	2562.0	.9983	2652.0	.0074		
2474.0	.5318	2564.0	.9999	2654.0	.0067		
2476.0	.5781	2566.0	.9985	2656.0	.0059		
2478.0	.6246	2568.0	.9970	2658.0	.0051		
2480.0	.6512	2570.0	.9955	2660.0	.0043		
2482.0	.6720	2572.0	.9940	2662.0	.0036		
2484.0	.6881	2574.0	.9925	2664.0	.0029		

Appendix B

DETAILED ASSESSMENTS OF VAS ON GOES-4, -5 AND -6

Special datasets were collected during the VAS postlaunch checkout periods in order to assess the zero-point, random noise, droop and spin-to-spin reproducability of the radiances.

The VAS-D instrument was launched on GOES-4 in September 1980. Even though the upper large detector was not functioning, the instrument was launched in order to backup VISSR operations. The VAS ground system was operating adaquately by November 1980, until the spring of 1981, and software was not complete until the autumn of 1981. VAS test datasets were acquired through September 1981, when GOES-4 was dedicated to VISSR operations in the GOES-WEST location at 135°W. GOES-4 failed prematurely in November 1982, due to loss of control of the scan mirror. The test data from VAS-D used in this report was collected on 18 February 1981. The previously reported assessment of VAS-D (Chesters, et al., 1981) was based upon the first orderly radiances collected in November 1980. The February 1981 data was collected with systematic radiance assessment in mind: 9 spins were taken in all 12 channels for several scan lines. The results from both time periods are essentially the same, which implies good seasonal stability for the VAS radiometer. The upper large detectors never functioned on GOES-4, and the S/DB software for the small detectors was not debugged in time for their evaluation.

VAS-E was launched on GOES-5 in May 1981. VAS data was taken experimentally from July through September 1981, when GOES-5 was dedicated to VISSR operations as GOES-EAST, located at 75°W, where it remains at this writing. On 4 August 1981, with GOES-5 stationed at 98°W, the VAS instrument was programmed with two Processor Data Loads (PDLs) for 9 spins per line over all 12 channels, exercising every possible filter/detector option. On GOES-5, the errors in both detectors were very similar for all bands.

VAS-F was launched on GOES-6 in April 1983. VAS data was taken experimentally for a only a few days in May 1983. The VAS instrument and ground system were being rushed into operation at this time. GOES-6 was dedicated to VISSR operations as GOES-WEST, in June 1983, where it remains at this writing. Radiometric test data consisting of 9 spins in all 12 channels, using the large and small detectors, were taken on 24 May 1983, with GOES-6 stationed at 135°W longitude. The errors listed for GOES-6 are dominated by a noisy lower large longwave detector.

The VAS channels operate with detector pairs, producing an "upper" and "lower" scanline with each spin. Postlaunch performance appraisals for every filter/detector combination on GOES-4, -5 and -6 are presented in the following tables. Section 4 describes the data reduction methods and summarizes the results with a single value for each kind of error for each channel.

TABLE 23

Radiance errors for VAS-D on GOES-4

Chan Up/Lo	Space Mean	Space Stdev.	W-E Droop	Spin/spin Reproducability
Large Detectors (erg/etc.)				
1 U	n.a.	n.a.	n.a.	n.a.
L	+0.6	±4.4	-0.5	±1.2
2 U	n.a.	n.a.	n.a.	n.a.
L	+0.7	±2.6	+1.0	±1.5
3 U	n.a.	n.a.	n.a.	n.a.
L	-0.1	±1.5	+1.1	±0.5
4 U	n.a.	n.a.	n.a.	n.a.
L	-0.0	±1.4	+0.4	±0.5
5 U	n.a.	n.a.	n.a.	n.a.
L	-0.2	±1.2	+0.2	±0.5
6 U	n.a.	n.a.	n.a.	n.a.
L	+0.006	±0.031	-0.006	±0.005
7 U	n.a.	n.a.	n.a.	n.a.
L	-0.2	±0.9	-0.4	±0.4
8 U	n.a.	n.a.	n.a.	n.a.
L	-0.3	±0.2	-0.2	±0.1
9 U	n.a.	n.a.	n.a.	n.a.
L	+0.1	±1.2	-0.1	±0.5
10 U	n.a.	n.a.	n.a.	n.a.
L	+0.1	±0.3	+0.0	±0.1
11 U	n.a.	n.a.	n.a.	n.a.
L	+0.003	±0.030	+0.000	±0.006
12 U	n.a.	n.a.	n.a.	n.a.
L	-0.002	±0.008	-0.002	±0.001
Small Detectors (erg/etc.)				
3 U	n.a.	n.a.	n.a.	n.a.
L	n.a.	n.a.	n.a.	n.a.
4 U	n.a.	n.a.	n.a.	n.a.
L	n.a.	n.a.	n.a.	n.a.
5 U	n.a.	n.a.	n.a.	n.a.
L	n.a.	n.a.	n.a.	n.a.
7 U	n.a.	n.a.	n.a.	n.a.
L	n.a.	n.a.	n.a.	n.a.
8 U	-0.5	±0.4	-0.5	n.a.
L	-0.2	±0.4	-0.3	n.a.
9 U	n.a.	n.a.	n.a.	n.a.
L	n.a.	n.a.	n.a.	n.a.
10 U	n.a.	n.a.	n.a.	n.a.
L	n.a.	n.a.	n.a.	n.a.

TABLE 24

Radiance errors for VAS-E on GOES-5

Chan Up/Lo	Space Mean	Space Stdev.	W-E Droop	Spin/spin Reproducability
Large Detectors (erg/etc.)				
1 U	+0.8	±2.7	-0.0	±0.7
L	+0.6	±2.8	-0.8	±1.7
2 U	+0.5	±1.5	+0.7	±0.4
L	-0.0	±1.5	+0.2	±0.3
3 U	+0.4	±1.0	+0.4	±0.3
L	+0.2	±1.1	+0.7	±0.5
4 U	-0.5	±0.9	-0.6	±0.3
L	+0.3	±0.9	+0.3	±0.4
5 U	+0.1	±0.8	-0.0	±0.2
L	-0.6	±0.8	-0.4	±0.3
6 U	+0.008	±0.022	+0.022	±0.018
L	+0.000	±0.023	-0.006	±0.001
7 U	-0.4	±0.6	+0.3	±0.1
L	-0.1	±0.8	-0.1	±0.2
8 U	+0.0	±0.1	-0.0	±0.1
L	-0.0	±0.2	-0.1	±0.3
9 U	+0.1	±0.5	-0.1	±0.1
L	-0.1	±0.6	-0.2	±0.2
10 U	-0.0	±0.2	-0.0	±0.0
L	-0.0	±0.2	+0.0	±0.0
11 U	+0.009	±0.027	+0.018	±0.006
L	+0.000	±0.024	+0.005	±0.006
12 U	+0.002	±0.007	+0.002	±0.005
L	+0.001	±0.007	+0.001	±0.003
Small Detectors (erg/etc.)				
3 U	-0.4	±2.5	-0.9	±2.8
L	+0.5	±2.0	-0.0	±2.7
4 U	+1.3	±1.9	+1.1	±0.9
L	+1.9	±1.9	-0.9	±0.5
5 U	-1.2	±1.5	-0.8	±0.4
L	+1.1	±1.3	-0.8	±0.5
7 U	-0.1	±1.4	-0.6	±0.5
L	-0.4	±1.3	-1.3	±0.6
8 U	-0.3	±0.3	-0.2	±0.1
L	+0.9	±0.3	-0.1	±0.1
9 U	+0.1	±1.2	-0.5	±0.6
L	+0.3	±1.3	+0.5	±0.5
10 U	-0.2	±0.3	+0.0	±0.2
L	+0.0	±0.3	+0.1	±0.2

TABLE 25

Radiance errors for VAS-F on GOES-6

Chan Up/Lo	Space Mean	Space Stdev.	W-E Droop	Spin/spin Reproducability
Large Detectors (erg/etc.)				
1 U	-0.3	±2.7	+1.5	±0.8
L	+0.3	±2.8	-0.3	±1.3
2 U	-0.5	±1.8	+0.5	±0.6
L	+0.4	±1.8	-1.4	±0.8
3 U	+0.4	±1.4	+0.0	±0.4
L	+0.1	±1.4	+0.8	±0.7
4 U	+0.6	±1.1	+1.2	±0.3
L	+0.2	±1.2	+1.6	±0.7
5 U	+0.6	±0.7	+1.3	±0.4
L	+0.4	±0.7	+0.0	±0.8
6 U	+0.002	±0.021	+0.004	±0.003
L	+0.000	±0.021	-0.002	±0.003
7 U	+0.2	±0.8	+0.6	±0.2
L	+0.1	±0.9	-0.2	±1.0
8 U	+0.0	±0.3	+0.1	±0.0
L	+0.0	±0.2	+0.0	±0.1
9 U	-0.1	±0.7	+0.5	±0.1
L	+0.1	±0.7	+0.5	±0.5
10 U	+0.1	±0.2	+0.2	±0.1
L	+0.1	±0.2	-0.3	±0.1
11 U	+0.010	±0.021	-0.012	±0.004
L	-0.002	±0.023	-0.018	±0.004
12 U	-0.001	±0.008	-0.000	±0.002
L	+0.000	±0.009	-0.002	±0.003
Small Detectors (erg/etc.)				
3 U	+0.6	±2.4	+0.6	±0.6
L	+1.0	±2.4	-1.0	±0.4
4 U	-1.4	±2.1	-0.0	±0.5
L	+0.5	±1.8	+0.8	±0.3
5 U	+0.6	±1.4	+1.3	±0.4
L	+0.7	±1.6	+0.7	±0.3
7 U	-0.5	±1.5	+0.3	±0.5
L	+0.3	±1.3	+0.5	±0.4
8 U	+0.0	±0.3	+0.0	±0.0
L	-0.1	±0.3	-0.0	±0.1
9 U	+0.3	±1.2	-0.5	±0.3
L	+0.3	±1.1	+0.3	±0.1
10 U	+0.1	±0.3	-0.0	±0.1
L	-0.1	±0.3	-0.0	±0.1

Appendix C

REFERENCES

Anon., 1978a: GSFC SVAS Ground Station Report. Westinghouse Electric Corporation, Defense and Electronic Systems Center, Command and Control Division, Baltimore, MD 21203. (Report FIS-78-4044 under contract NAS 5-24306).

----, 1978b: VAS S/DB Calibration Parameter Definition. ibid., (Contract NAS 5-23582).

----, 1979a: Wallops VAS S/DB Mode AA Output Format (Revision B). ibid..

----, 1979b: GSFC VAS PreProcessor Data Formats (Revision D). ibid..

----, 1979c: GSFC VAS PreProcessor Real Time Software (Revision A). ibid..

----, 1979d: GSFC VAS PreProcessor Off Line and Test Simulator Software. ibid..

----, 1979e: Synchronizer Data Buffer System Design Report for the CDA Station. ibid..

----, 1980: VAS Preprocessor Software Manual. ibid..

Bristor, C.L., 1975: Central processing and analysis of geostationary satellite data. NOAA TM NESS-64. 155 pp.

Burch, D.E., D.A. Gryvnak and J.D. Pembrook, 1970: Investigation of the absorption of infrared radiation by atmospheric gases. AFCRL-70-0373 (NTIS-70N42640).

Burch, D.E., D.A. Gryvnak and J.D. Pembrook, 1971: Investigation of the absorption of infrared radiation by atmospheric gases: water, nitrogen, nitrous oxide. AFCRL-71-0124 (NTIS-71X78131).

Chesters, D., L.W. Uccellini, H.E. Montgomery, A. Mostek and W. Robinson, 1981: Assessment of the first radiances received from the VISSR Atmospheric Sounder (VAS) instrument. NASA TM 83827 (NTIS-82N19730).

Chesters, D., L.W. Uccellini and A. Mostek, 1982: VISSR Atmospheric Sounder (VAS) Simulation Experiment for a Severe Storm Environment. Monthly Weather Review, 110, 198-216.

Chesters, D., L.W. Uccellini and W. Robinson, 1983: Low-level water vapor fields from the VISSR Atmospheric Sounder (VAS) split window channels. Journal Climate and Applied Meteorology, 22, 725-743.

Chesters, D., W.P. Menzel, H.E. Montgomery and W.R. Robinson, 1984: VAS Instrument Performance Appraisal. Final Report of the VAS Demonstration, ed. H.E. Montgomery and L.W. Uccellini. (In preparation).

Greaves, J.R., H.E. Montgomery, L.W. Uccellini and D.L. Endres,

Gatlin, J.A., 1982: Correlation of 3-hour radiosonde data with coincident NIMBUS-7 total ozone measurements. VISSR Atmospheric Sounder (VAS) Research Review, 1983: ed. J.R. Greaves. NASA CP-2253 (NTIS-83N24028), pp 31-33. 1982: 1982 AVE/VAS ground truth field experiment: satellite data acquisition summary and preliminary meteorological review. NASA/GSFC X-903-82-17.

Greaves, J.R., editor, 1983: VISSR Atmospheric Sounder (VAS) Research Review. NASA CP-2253 (NTIS-83N24028).

Lee, T.H., D. Chesters, and A. Mostek, 1983: The Impact of Conventional Surface Data Upon VAS Regression Retrievals in the Lower Troposphere. Accepted by Journal Climate and Applied Meteorology. (NASA TM 83987 and NTIS-83N27522).

Malinowski, F.R. and R.D. Ruiz, 1980: VAS-D GOES Data Book (2 volumes). Santa Barbara Research Center, Hughes Aircraft Co., 75 Coromar Drive, Goleta, CA 93017 (Contract NAS 5-20769).

McClatchey, R.A., W.S. Benedict, S.A. Clough, D.E. Burch, R.F. Calfee, K. Fox, L.S. Rothman, and J.S. Garing, 1973: AFCRL atmospheric absorption line parameter compilation. AFCRL-TR-73-0096 (NTIS-73N30382).

Menzel, W.P., 1980: Prelaunch Study Report of VAS-D Performance. University of Wisconsin, Space Science and Engineering Center, 1225 West Dayton Street, Madison, Wisconsin 53706 (Contract NAS 5-21965).

----, 1981a: Postlaunch Study Report of VAS-D Performance. ibid..

----, 1981b: Prelaunch Study Report of VAS-E Performance. ibid..

----, 1981c: Postlaunch Study Report of VAS-E Performance. ibid..

----, 1983a: Prelaunch Study Report of VAS-F Performance. ibid..

----, 1983b: Postlaunch Study Report of VAS-F Performance. ibid..

Menzel, W.P., W.L. Smith and L.D. Herman, 1981: Visible infrared spin-scan radiometer atmospheric sounder radiometric calibration: an

inflight evaluation from intercomparisons with HIRS and radiosonde measurements. Applied Optics, 20, 3641-3644.

Menzel, W.P., W.L. Smith and T.R. Stewart, 1983a: Improved cloud motion wind vector and altitude assignment using VAS. Journal of Climate and Applied Meteorology, 22, 377-384.

Menzel, W.P., W.L. Smith, G.S. Wade, L.D. Herman and C.M. Hayden, 1983b: Atmospheric soundings from a geostationary satellite. Applied Optics, 22, 2686-2689.

Montgomery, H.E., 1980: Execution Phase Project Plan for Operational Satellite Improvement Program Plan - VISSR Atmospheric Sounder (VAS) Demonstration (Revision 2). NASA/GSFC Management Copy.

Montgomery, H.E. and D.K. Endres, 1977: Survey of dwell sounding for VISSR Atmospheric Sounder (VAS). NASA/GSFC X-942-77-157.

Roberts, R.E., J.E.A. Selby, and L.M. Biberman, 1976: Infrared continuum absorption by atmospheric water vapor in the 8 to 12 micron window. Applied Optics, 15, 2085-2090.

Smith, W.L., V.E. Soumi, W.P. Menzel, H.M. Woolf, L.A. Sromovsky, H.E. Revercomb, C.M. Hayden, D.N. Dickson and F.R. Mosher, 1981: First sounding results from VAS-D. Bulletin American Meteorology Society, 62, 232-236.

Smith, W.L., 1983: The retrieval of atmospheric profiles from VAS geostationary radiance observations. Journal of Atmospheric Sciences, 40, 2025-2035.

Szejwach, G., 1982: Analysis of multispectral data using an unsupervised classification technique -- application to VAS. VISSR Atmospheric Sounder (VAS) Research Review, 1983: ed. J.R. Greaves. NASA CP-2253 (NTIS-83N24028), pp 11-12.